Renewable based thermal systems for microgrids

Mariana Almeida Garcia da Silva

Thesis to obtain the Master of Science Degree in

Mechanical Engineering

Supervisors: Prof. Carlos Augusto Santos Silva
Dr. Jorge Manuel Resende Vieira Facão

Examination Committee

Chairperson: Prof. Edgar Caetano Fernandes
Supervisor: Prof. Carlos Augusto Santos Silva
Member of the Committee: Prof. Luís Filipe Moreira Mendes

December 2021

ACKNOWLEDGEMENTS

First, I wish to thank Prof. Carlos Augusto Silva for the constant help and motivation throughout this thesis. Also, I am grateful to Prof. Jorge Facão for his assistance, as an important connection to LNEG.

I would like to thank my family for their constant support throughout my life, and especially in this thesis. The education they have provided me was fundamental to successfully completing this course, and the example they give me every day is an incredible inspiration.

Finally, I would like to thank my friends for their company, patience, and for always encouraging me whenever I needed it most; helping me overcome all the obstacles faced in the last 5 years. They are responsible for the best memories of my time at university.

ABSTRACT

Buildings have a significant contribution to the total energy consumption in the world, playing, therefore, an important role in reaching a more decarbonized and efficient energy sector. Space heating and cooling represent a large portion of the energy consumption in buildings, making the development and improvement of energy systems for these activities crucial. A system for space heating/cooling using solar energy and atmospheric air as heat sources was modeled in Simulink. The main elements of the system were a solar collector, a hot water tank, a storage tank, fan coils, and an air-water heat pump. The system was tested in both winter and summer, and parametric studies were done to improve its performance. The results obtained were promising, as the system was able to keep the spaces in the considered comfort zone for the majority of the time (less than 2% of discomfort hours in the winter, and less than 10% in the summer in Lisbon). A modification in the location of the system was also done, from Lisbon to Madrid.

Key-words: energy, Solar energy, Heat pump, Space heating and cooling, Simulink

RESUMO

Os edifícios têm uma contribuição significativa para o consumo total de energia no mundo, desempenhando, um papel importante para alcançar um sector energético mais descarbonizado e eficiente. O aquecimento e arrefecimento dos espaços representam uma parte considerável do consumo de energia nos edifícios, tornando crucial o desenvolvimento e melhoria de sistemas para estas actividades. Um sistema de aquecimento/arrefecimento de espaços utilizando energia solar e ar atmosférico como fontes de calor foi modelado em Simulink. Os principais elementos do sistema foram um colector solar, dois tanques de água, *fan coils* e uma bomba de calor ar-água. O sistema foi testado tanto no Inverno como no Verão, e foram feitos estudos paramétricos para tentar melhorar o seu desempenho. Os resultados obtidos foram promissores, uma vez que o sistema conseguiu manter os espaços na zona de conforto considerada durante a maior parte do tempo (menos de 2% das horas de desconforto no Inverno, e menos de 10% no Verão em Lisboa). Foi também feita uma modificação na localização do sistema, de Lisboa para Madrid.

Palavras-chave: energia, energia solar, bomba de calor, aquecimento e arrefecimento de espaços, Simulink

Table of Contents

LIST OF TABLES

LIST OF FIGURES

LIST OF ABBREVIATIONS

HVAC	Heating, Ventilation, and Air Conditioning
PNEC	Plano Nacional Energia e Clima
nZEB	Nearly Zero-Energy Buildings
LNEG	Laboratório Nacional de Energia e Geologia
HP	Heat Pump
SAHP	Solar Assisted Heat Pump
DX-SAHP	Direct Solar Assisted Heat Pump
IDX-SAHP	Indirect Solar Assisted Heat Pump
AWHP	Air-water Heat Pump
COP	Coefficient of Performance
MPC	Model Predictive Control
RMSE	Root Mean Square Error

LIST OF SYMBOLS

A_c	Area of the collector
A_{fc}	Area of the contact of the water and air in the fan coil
A_{loss}	Area of the tank in contact with the room
A_o	Area used for the losses in the fan coil
A_{coil}	Area of the coil heat exchanger
A_{ext}	Area in contact with the exterior
c_{p_a}	Air heat capacity
c_{p_w}	Water heat capacity
h	Heat transfer coefficient for losses in the fan coil
I	Irradiance
k_{j1}	Thermal conductivity (layer below in the tank)
k_{j2}	Thermal conductivity (layer above in the tank)
N_r	Number of rooms in contact with Room i
$\dot{Q}_c$	Useful heat in the solar collector
$\dot{q}$	Heat generated inside the building
s_1	Size variable for the temperature
s_2	Size variable for the variation of flowrate
T_{cin}	Inlet temperature of solar collector
T_{cout}	Outflow temperature of solar collector
T_{tout}	Outflow temperature of the hot water tank
T_a	Ambient temperature
T_j	Temperature of the layer of the tank considered
T_{j-1}	Temperature of the layer above in the tank
T_{j+1}	Temperature of the layer below in the tank
T_{wout}	Outflow temperature of the water in the fan coil
T_{win}	Inlet temperature of the water in the fan coil
T_i	Temperature of Room i
T_k	Temperature of the Room k, in contact with room i
T_{aout}	Outflow temperature of the air in the fan coil
T_{ain}	Inlet temperature of the air in the fan coil
$T_{aout(i)}$	Outflow temperature of the air in the fan coil i
T_{cini}	Temperature of the fluid inside the coil part in contact with layer j
T_{ref}	Reference temperature

U_{coil}	Overall heat transfer coefficient in the coil heat exchanger
U_{fc}	Overall heat transfer coefficient of the fan coil
U_{loss}	Overall heat transfer coefficient for the losses to the room
U_{ext}	Overall heat transfer coefficient for the losses with the exterior
U_{L1}, U_{L2}	Overall heat transfer coefficients for losses in the solar collector
V_a	Volume of air in the fan coil
V_w	Volume of water in the fan coil
V_{tank}	Volume of the layer of the tank
V_i	Volume of Room i
$\dot{V}_{vent}$	Volumetric flowrate of ambient air for ventilation
$\dot{V}_c$	Solar system volumetric flowrate
$\dot{V}_a$	Volumetric flowrate of air in the fan coil
$\dot{V}_w$	Volumetric flowrate of water in the fan coil
$\dot{V}_t$	Hot water volumetric flowrate from the tank
$\dot{V}_{HVAC}$	Volumetric flowrate of air from the fan coil
$\dot{V}_{c(t)}$	Solar system flowrate for the current time step
$\dot{V}_{c(t-1)}$	Solar system flowrate for the previous time step
w_1	Weight of the temperature
w_2	Weight of the variation of flowrate
Δx	Height of the layer
Δ	Tunable constant for stratification
η_0	Zero loss collector efficiency
ρ_a	Air density
ρ_w	Water density

1 Introduction

1.1 Motivation

Climate change and the increase of carbon emissions are forcing immediate modifications in the energy sector, emphasizing the need for an energy transition. This energy transition aims at decreasing carbon emissions by reducing fossil fuel-based energy sources and by increasing the share of renewable energy. Along with this transition, it is essential to decrease the energy consumed in the world.

The energy consumption of buildings represents approximately 40% of the final energy consumption in Europe and 30% in Portugal [1]. Space and water heating, space cooling, and appliances are the main consumers in the building sector, changing their importance depending on residential or commercial buildings or climate. To reduce the energy consumption in buildings, energy efficiency measures are crucial.

Energy efficiency can reduce more than 50% of the energy consumption in buildings in Portugal [1]. Improving lighting, HVAC systems, or thermal isolation of buildings are some energy efficiency measures that can be implemented.

In Portugal, the National Energy and Climate Plan (PNEC 2030) [2] defines the objectives and targets for the next years. Examples are a 45% to 55% reduction of emissions (in comparison to 2005 without land use, land-use change, and forestry), a 35% increase in energy efficiency (% reduction in primary energy consumption), or a 47% share of renewable energy. One of the objectives of this plan is the rehabilitation and renovation of buildings increasing their energy efficiency.

PNEC 2030 also promotes the implementation of nearly zero-energy buildings (nZEB) in Portugal in the next ten years. Nearly zero-energy buildings are buildings with very high energy performance, in which the low energy consumed must originate mainly from renewable energy sources.

1.2 Objectives

The objective of this thesis is to develop a thermal model in Simulink for space heating/cooling that integrates renewable energy in a building at Laboratório Nacional de Energia e Geologia (LNEG). This model will be applied in LNEG to control the system in real time. This thesis is incorporated in the IMPROVEMENT research project aiming at transforming public buildings in nZEB using microgrids that include renewable energy, combined heat, cold, and electricity generation, and energy storage [3]. Microgrids are local energy systems that integrate energy generation sources and loads and can be disconnected from the grid, operating independently, being important to incorporate renewable energy.

1.3 Contributions

- Validation of previous models
- Development of a heat pump model
- Modeling of an integrated thermal system
- Application of control strategies
- Contribution to a paper being prepared in collaboration with members of the IMPROVEMENT project, where the validation process and models developed in this thesis are included.

1.4 Structure of the thesis

This thesis is organized into six chapters. Chapter 1, which is the current chapter, contextualizes the thesis and includes an introduction. Chapter 2 presents the literature review and the state of the art of the energy systems studied, while Chapter 3 defines the case study analyzed. In Chapter 4, the methodology and modeling used are explained in detail, with the results presented and discussed in Chapter 5. Chapter 6 presents the conclusions and recommendations for future work.

2 Literature review

2.1 Background

2.1.1 Solar thermal

Solar thermal systems convert solar energy into heat and represented 7% of the global renewable heat consumption in 2018 [4]. The main application of these systems is domestic water heating in single-family houses, which represents 53% of the total installed water collector capacity in operation by the end of 2018 [5]. Water heating in multi-family houses, tourism, and in the public sector represented 37% and solar combined systems in buildings, supplying hot water and space heating, represented only 2% of the total installed capacity.

In contrast with small-scale solar thermal heating systems that are losing market share, the number of large-scale systems has been increasing significantly in the last years [5], as represented in Figure 1.

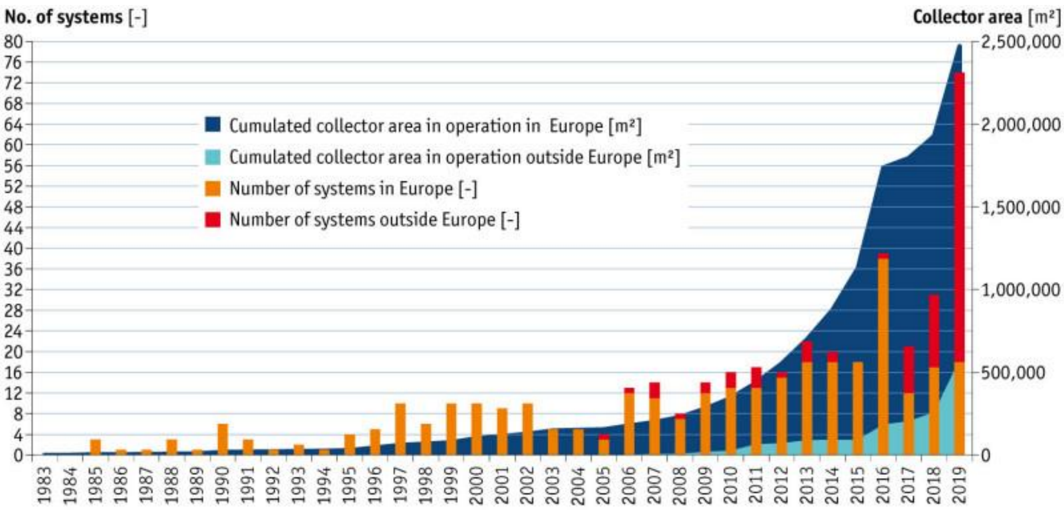

Figure 1 – Annual achievement and cumulated area in operation in 2019 of large-scale heating systems [5]

Portugal has high irradiance levels making solar thermal systems a suitable technology for heat production. In 2018, solar thermal systems in Portugal produced 74.7 KWth per 1000 capita [6].

Traditionally, the main components of solar thermal systems are a solar collector, a storage tank, and a backup system.

Solar collectors are the key components of the system and their function is to absorb solar radiation and use it to heat a fluid that circulates inside. According to [5], the most common solar collectors are evacuated tubes (70.4%), flat plate (22.6%), and unglazed water collectors (6.1%). There are also collectors with air as the working fluid, but they represent a minority.

Storage tanks heat or cool the medium inside, store thermal energy, and are important to detach the production of renewable energy from the heating or cooling demand. Water is the most used medium for storage tank systems because it has a high specific heat capacity, chemical stability, and availability, and a low price [7].

Backup systems are auxiliary heating devices used to supply heat when solar radiation is not available or it is insufficient. These devices can be included in the storage tank, for example, as an electrical resistance.

Solar thermal systems have two working principles that are represented in Figure 2: Thermosiphon and forced-circulation. Thermosiphon systems work by gravity, as a result of the different densities associated with the temperature of the fluid. The hot water rises and accumulates in the tank whereas the cold water passes in the collector where it is heated. This working principle is more common for houses in hot climates and represents 58% of the global installed solar thermal systems [5].

Forced-circulation systems transport the working fluid between the solar collector and the tank using a pump, allowing for an improved performance of the system. An important advantage of this system is the capacity to control the pump based on the temperature difference between the solar collector and the tank.

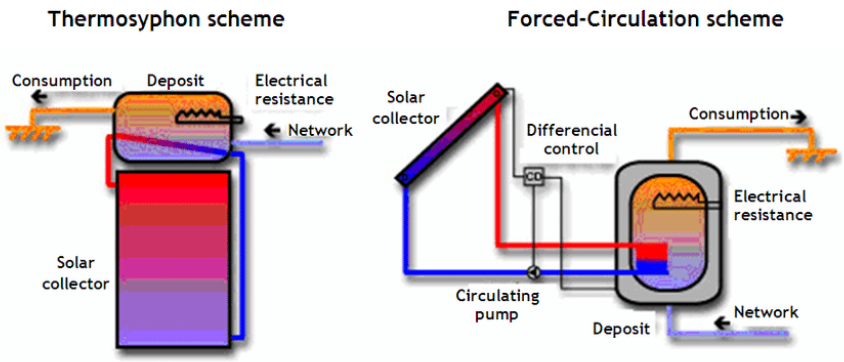

Figure 2- Schemes of thermosiphon and forced-circulation solar thermal systems [8]

The combination of solar thermal and other heating technologies such as heat pumps is supported worldwide. In Portugal, PNEC 2030 refers that “In buildings, the solar thermal should coexist with other technologies of great potential and efficiency, such as biomass boilers and heat pumps. Still, it will maintain a significant role in the preparation of hot water, and in addition to other efficient solutions, it presents itself as one of the most efficient ways for space and water heating, contributing to the increase of comfort.”

2.1.2 Heat pump

Heat Pumps are devices that transfer heat from a low temperature to a high temperature source using external energy. Space heating, water heating, and space cooling for residential and commercial buildings are some applications of heat pumps, but these devices are also important in industrial processes.

The working principle of heat pumps is based on a refrigerant cycle. Figure 3 represents the cycle performed by the refrigerant, which has four different phases: compression, condensation, evaporation, and expansion. In the evaporator, the refrigerant receives the heat from the source and changes into a gaseous state at a low temperature, whereas in the condenser the refrigerant returns to a liquid state and releases heat for the high temperature source.

In the compression phase, both the pressure and the temperature of the refrigerant increase. This phase can be performed either by mechanical compression (mechanical heat pump) or by a thermally driven compression (absorption heat pump).

The heat pump can operate in heating mode with the building receiving heat from the condenser. If instead, the space had a cooling demand, the building would supply heat to the evaporator and the condenser would release the heat to the medium used. This switch between heating and cooling modes with the same device is possible using a reverse valve in the heat pump.

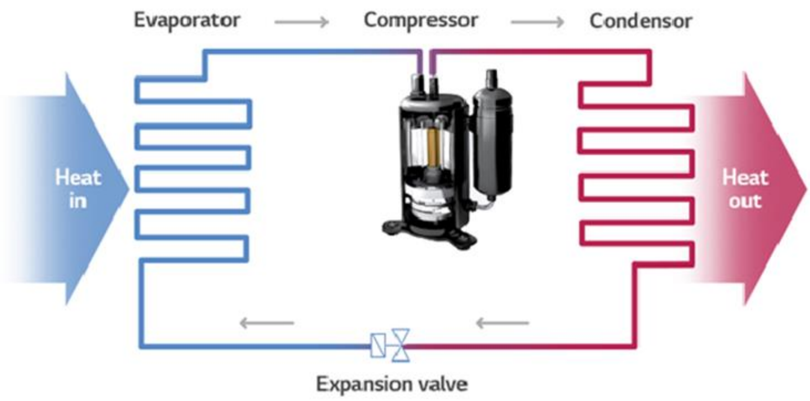

Figure 3- Heat Pump working cycle, Adapted from [9]

The most common heat sources used in heat pumps are air, water, and ground. Figure 4 represents the sales of heat pumps in the EU by source. In 2018, air to air was the dominant source for heat pumps with approximately 608 thousand units sold [10]. These devices transfer heat between the atmosphere and the indoor air.

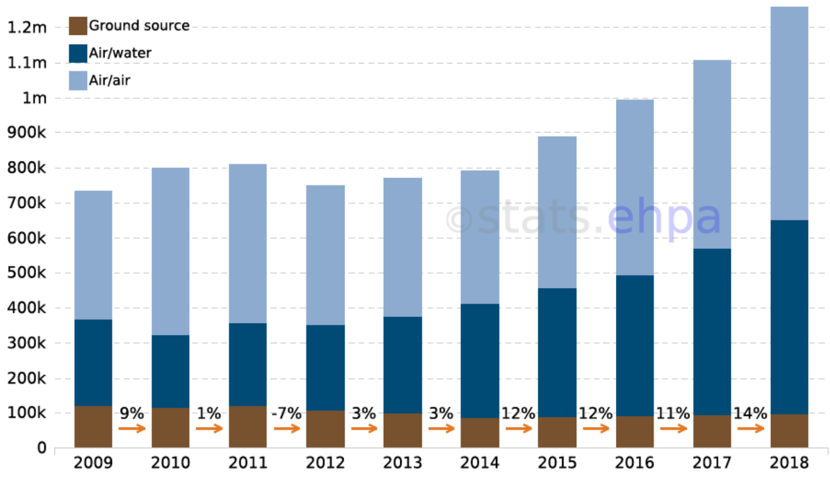

Figure 4-Sales of heat pumps by source [10]

As indicated in Figure 4, the sales of heat pumps have been growing in the last years. This can be partially explained by the necessity of reducing carbon emissions. Heat pumps, when used with renewable heat and compression sources, do not release CO2 and therefore can help to decarbonize the heating and cooling sectors. In the EU, heat pumps are responsible for an annual reduction of 9.16 million tons of CO2[11].

Heat pumps have also other important contributions for the energy sector, such as the reduction of energy consumption and energy dependency. The contribution of heat pumps in heating in Portugal has decreased the energy dependency by 2% in 2019 [12].

2.2 State of the art

2.2.1 Solar thermal assisted heat pump

Solar assisted heat pumps (SAHP) integrate solar thermal systems with heat pumps. These systems have gained importance in the last years because of the advantages when compared to both technologies separated. SAHP can be direct (DX-SAHP) and indirect (IDX-SAHP).

In DX-SAHP, both the solar thermal and heat pump systems belong to the same system, and the refrigerant passes directly in the solar collector, acting as an evaporator (see Figure 5). The heat is provided by solar radiation and/or ambient air [13].

DX-SAHP has advantages when compared to solar thermal and heat pumps separated. The circulation of the refrigerant in the collector reduces the heat losses and DX-SAHP has a higher evaporating temperature [14].

Several studies involving DX-SAHP are available in the literature. In addition to the collector/solar evaporator, [15] used an evaporator with atmospheric air as the heat source. The authors studied the influence of the irradiance and ambient temperature in the different configurations of the solar and air evaporators.

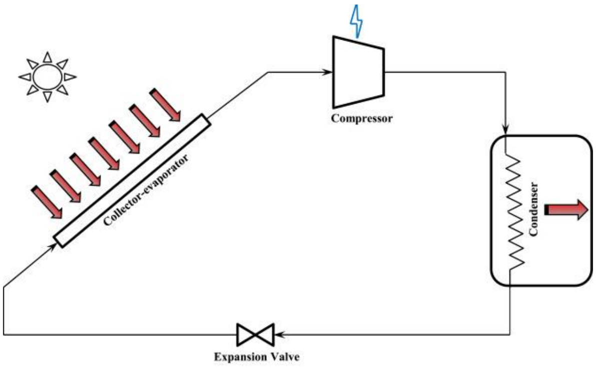

Figure 5-Direct Solar Assisted Heat Pump [13]

Indirect solar-assisted heat pumps have three types of standard configurations: Parallel, Series, and Dual, which are represented in Figure 6.

The parallel configuration has separated loops for the solar thermal and heat pump systems. The solar thermal system runs when solar radiation is enough to fulfill the demand, otherwise, the heat pump is switched on [16]. Parallel systems have advantages over other SAHP. They are, for example, more robust and reliable than Series SAHP [17].

In Series SAHP, the solar collectors are the heat source of the heat pump. There are differences in the definition of Series SAHP in the literature. [18] considers that when the solar thermal is enough, the heat pump can be bypassed, while in [16] the heat pumps works always in combination with the solar thermal system.

Dual-source heat pumps have two heat sources. One of the main types found in the literature is the dual solar-ground HP, which combines solar energy and energy from the ground and has had considerable research in the past years.

Concerning the coupling of ground heat pumps and solar thermal systems, [19] divides the studies previously performed into three strategies, depending on the type of usage of the soil. The first strategy uses the ground only as heat source, the second as the heat source and short-term storage, and the last one as the heat source and seasonal heat storage.

In the past years, different systems have been created that are a combination of the previous configurations, or even more complex. The use of two tanks has been a common increase in the complexity of the system found in the literature. For example [20] and [21] investigated a model with two tanks, one for domestic hot water (DHW) use and another, called Float Tank, that could float in temperature and absorb more solar energy.

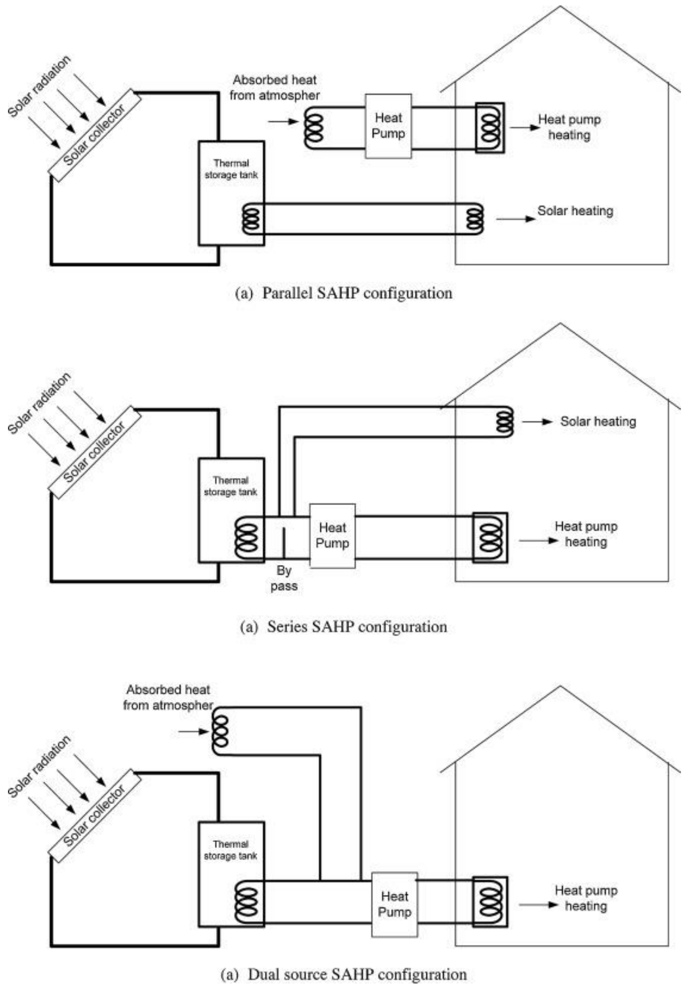

Figure 6-Indirect Solar Assisted Heat Pumps configurations [18]

2.2.2 Solar thermal assisted heat pump for space heating

The utilization of solar thermal assisted heat pumps for space heating has already been analyzed in the literature. [21] studied a SAHP system for space heating with two tanks. The heat pump was used to heat one of the tanks, which is then connected to a radiator. An energy saving of 20% could be obtained if this system was used as a retrofit in the existing Canadian houses.

[22] used a similar system with a water-water heat pump, auxiliary heaters, and two tanks, one of them a seasonal one. The study proved that the incorporation of the heat pump can improve the solar fraction of the system.

2.2.3 Solar thermal and Air-water heat pump

The combination of solar thermal and air-water heat pumps (AWHP) for space heating has been analyzed in several studies to combine solar and atmospheric heat. [23] studied a system with an AWHP and a solar collector connected in parallel to a buffer tank. The AWHP had the evaporator in contact with the ambient air and the condenser in contact with the water. The AWHP was activated at low solar radiation, being a fundamental heat source, as the solar system could not satisfy the total energy demand.

[24] investigated a system with solar collectors and an AWHP that could load the tank or provide direct space heating. An electrical auxiliary heater was used when the heat pump could not reach the necessary temperature. The study focused on the effect of component properties on the energy demand. A system with an AWHP and another with a ground source HP were compared, analyzing, for example, the effect of the size of the tank and solar heat exchanger on the electricity used.

2.2.4 Modeling

Different software tools are available and used for the modeling of energy systems. TRNSYS (Transient System Simulation Tool) is the most common software for modeling SAHP and its performance. Other software are Energy-Plus, ESP-r, Insel, and Matlab [25]. POLYSUN is also one of the most used commercial software and has already been validated in the literature [26]. For that reason, it was chosen as validation software for the work presented here.

TRNSYS is a software that allows simulating transient systems, including energy ones. This software has a library with approximately 150 components of different areas, being a flexible platform for building simulations [27]. It allows the incorporation of solar, HVAC, and building systems [28], but has only simple controllers, which can be a disadvantage [29].

Matlab/Simulink allows the implementation of a dynamic approach using modular systems. This flexibility is very useful because the system can be divided into modules representing each component, with the equations easily modeled using blocks or code. Matlab also has a lot of options to visualize the results and offers the possibility of future expansion and future control of the systems [30]. As Matlab/Simulink offers the possibility to create models, both for components and complex control and allows for real time control, it was the chosen software.

Matlab/Simulink was already used in the literature to model solar thermal systems for space heating. [31] developed a system with a solar collector, pumps, a thermal storage tank, a boiler, and a building, and [32] modeled a solar system and the inside of a greenhouse. Coupling the solar thermal system to heat pumps, [33] and [34] modeled a space heating system with a water-water heat pump and fan coils/radiators to transfer the heat from the water to the building. However, a gap in the literature was found for models coupling solar thermal and air-water heat pumps for space heating in Matlab/Simulink, being these systems already modeled in TRNSYS [35].

2.2.5 Control

Different strategies are available to control energy systems. The most used in the literature are the traditional: on-off and PID control, as well as, more advanced strategies such as Model Predictive Control (MPC).

On-off is a control strategy, where the controlled variable can only have two values: zero or its maximum value. When, for example, the controlled variable is the flowrate of a pump, the control switches on or off the pump, but cannot vary the value of the flowrate to an intermediate state. For the case of a pump in a thermal system, most cases found in the literature use a decision based on a temperature difference between two points, being called differential control. According to [36], on-off control has advantages compared to other strategies, such as its simplicity. However, it lacks the accuracy and efficiency of more advanced methods. [35] used on-off to control the three pumps of the system: the solar system pump, the pump for the heat pump, and the pump for the radiators. The decision was based on temperature differences in specific points.

In the PID control, the flowrate of the pump can be varied between zero and the maximum value. Although it is the most common control used, the PID parameters may be difficult to tune.

Model Predictive Control is a more advanced control strategy. Its principle is based on the optimization of the system, using a cost function. The decision of the controlled variable value is also based on the future predicted variables. This control strategy has several advantages, both related to control parameters (transient and steady response, multivariable control) and to the prediction of future control actions. The main disadvantages are the difficulty to create a model that can accurately represent the system and the cost of the installation [36]. [37] modeled a solar HVAC system and used MPC to control the two pumps of the system. For the optimization problem, the reduction of the energy consumed by the pumps and the proximity to the desired temperature differences were the criteria used.

3 Case study

This thesis is integrated into the IMPROVEMENT project, and specifically studies a building in Laboratório Nacional de Energia e Geologia (LNEG), also a member of this project. The building has a thermal system and an electric system to provide heat/cold and electricity. In this thesis, the thermal system and a specific part of the building were modeled, and tests were done to analyze the performance of the system and the comfort/discomfort obtained.

The building simulated in this thesis is represented in Figure 7 . It is composed of five rooms and an unconditioned area that was not modeled. Room 1 is a multiuse room with an area of $80m^2$, designed to accommodate eight people. Room 2 is used for meetings. It has $22m^2$ of area and is occupied by five people. Finally, Rooms 3, 4, and 5 are individual offices, each with an area of $11m^2$.

Regarding the exterior walls, the overall heat transfer coefficient was assumed to be between $0.5 - 1\ W/m^2K$, and the dimensions of the rooms were used to calculate the area in contact with the outdoor. For the interior walls, the overall heat transfer coefficient considered was $0.5W/m^2K$.

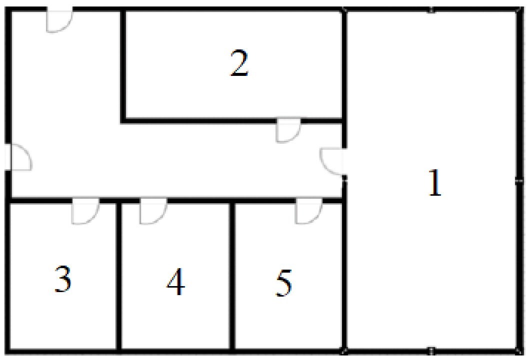

Figure 7 - Part of the building in LNEG studied, Adapted from [38]

The thermal system at the LNEG Pilot Plant consists of two solar collectors (with $2\ m^2$ each), a 300L tank, an air/water Heat Pump, a 1000L storage tank, and fan coils.

The weather files used for the simulation of the system in Simulink were downloaded from POLYSUN. The ambient temperature and the irradiance for Lisbon for three weeks in the month of January and July/August are represented in Figure 8 and Figure 9.

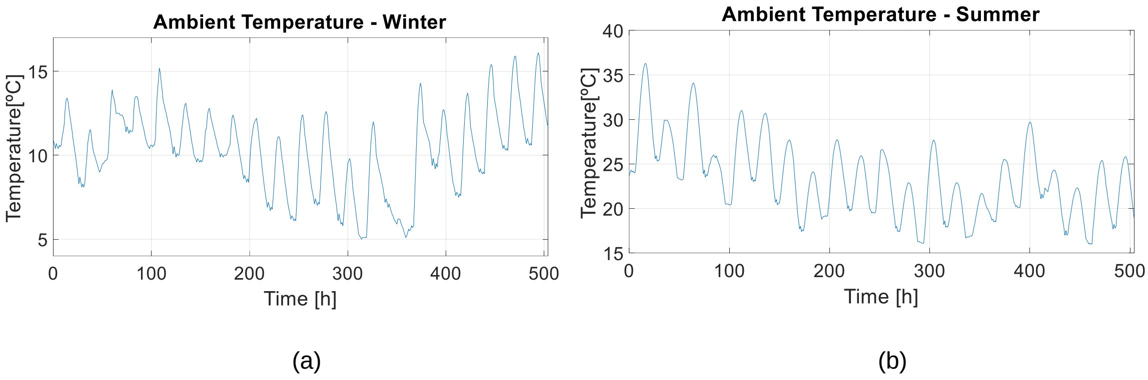

Figure 8 – Ambient temperature in Lisbon from POLYSUN, (a) Winter, (b) Summer

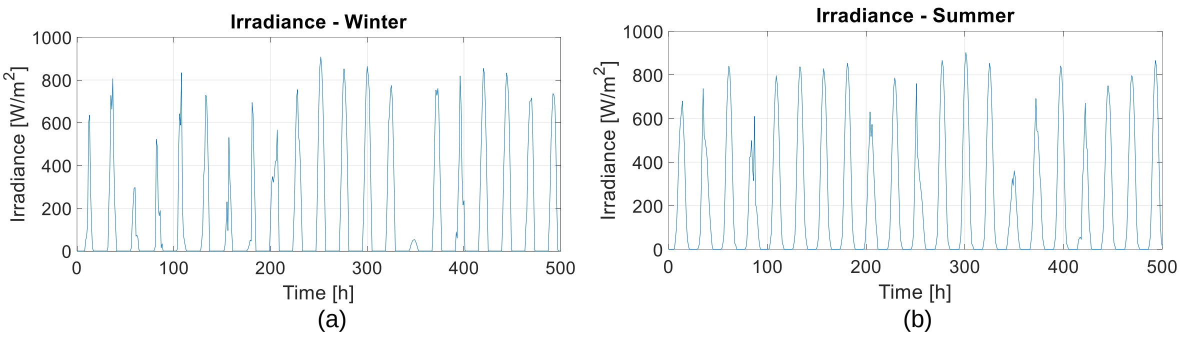

Figure 9 - Irradiance in Lisbon from POLYSUN, (a) Winter, (b) Summer

4 Methodology and Modeling

In this chapter, the procedure used to model each component will be explained, as well as the validation methodology of previous models. In addition, the configuration of the system implemented will be described, along with the strategies used for its control.

4.1 Validation

4.1.1 Solar collector and tank

4.1.1.1 Initial model

Previous models of the solar collector and the tank developed in [38] were used to simulate the system implemented in LNEG. These models required validation, to guarantee an accurate performance.

The initial model from [38] simulated a solar collector and a tank connected by a pump. When the pump is on, flowrate circulates in the system, going through the solar collector and the coil heat exchanger located inside the tank. The tank has one exit and one entry for hot water supply. The model followed Equation 4.1 for the outflow temperature of the solar collector, Equation 4.2 for the outflow temperature of the tank, and Equation 4.3 for the inlet temperature of the solar collector.

$$\rho c_p V \frac{dT_{cout}}{dt} = \dot{Q}_c \quad + \rho c_p \dot{V}_c (T_{cin} - T_{cout}) \tag{4.1}$$

$$\rho c_p V \frac{dT_{tout}}{dt} = \rho c_p \dot{V}_t (T_{tin} - T_{tout}) - U_{coil} A_{coil} (T_{tout} - T_{cin}) \tag{4.2}$$

$$\rho c_p V \frac{dT_{cin}}{dt} = \rho c_p \dot{V}_c (T_{cout} - T_{cin}) - U_{coil} A_{coil} (T_{cin} - T_{tout}) \tag{4.3}$$

The useful heat in the solar collector is given by:

$$\dot{Q}_c = A_c \eta_0 I - U_{L1} A_c \left(\frac{T_{cout} + T_{cin}}{2} - T_a\right) - U_{L2} A_c \left(\frac{T_{cout} + T_{cin}}{2} - T_a\right)^2 \tag{4.4}$$

4.1.1.2 New model

As will be discussed in Chapter 5, the model described above presented some limitations. Therefore, changes were performed in this work that are described below.

Solar collector

The temperature of the collector used in the loss term was changed with respect to Equation 4.1. The expression used in the models for the calculation of the temperature at the inlet of the solar collector is an energy balance at the exit of the coil of the tank. When the pump is on, no significant differences between the temperature at these two locations (exit of the coil of the tank and inlet of solar collector) arise. However, when the pump is off, T_{cin} is calculated as being in contact with the tank, and therefore, is at a temperature close to the temperature of the tank. As the temperature of the tank is usually high, the average between T_{cin} and T_{cout} (in contact with the solar collector) becomes high as well, increasing the losses of the solar collector to the atmosphere. However, the losses in the solar collector, are not able to decrease the temperature at the tank, keeping T_{cin} at the same values, despite the losses in the solar collector. This effect brings T_{cout}, to significantly low temperatures, as the losses are oversized. To solve this problem, when the pump was off, a different equation was implemented, which only considered T_{cout} for the losses term in the solar collector.

The new equation for the solar collector model when the pump is off is therefore:

$$\rho c_p V \frac{dT}{dt} = A_c \eta_0 I - U_{L1} A_c (T_{cout} - T_a) - U_{L2} A_c (T_{cout} - T_a)^2 + \rho c_p \dot{V}_c (T_{cin} - T_{cout}) \quad (4.5)$$

Tank

The new model accounts for the stratification of the tank, considering 12 layers, as it is the number of layers considered in POLYSUN. The important aspect of a stratified tank is that the layers at the top must have a higher temperature than the layers at the bottom. That effect was simulated based on [39]. If any layer at any time has a temperature higher than the layer above or lower than the layer below, a tunable constant Δ is set from zero to a value of a high order of magnitude to transfer the heat upwards and correct the situation.

As the layers with the highest/lowest temperatures are, respectively, the top/bottom layer, the new models consider that the outflow of the tank is at the top and that the return water enters the tank at the bottom layer.

The coil considered is in the middle of the tank, which affects layers 5 to 8, as represented in Figure 10. The water demand leaves the tank in layer 1 and returns cold to layer 12. The model considers that every layer receives a flowrate from the layer below when there is a hot water demand different from zero.

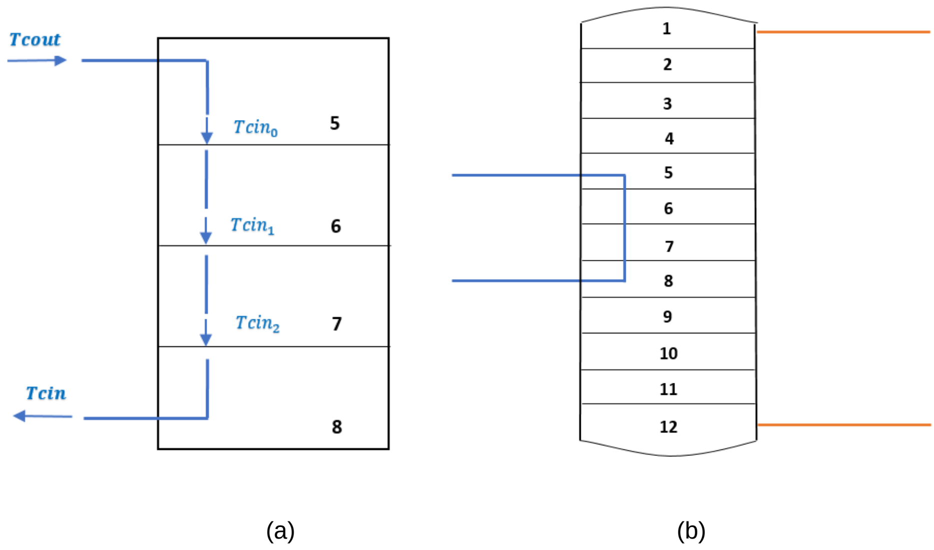

Figure 10 - Representation of the stratified tank model implemented, a) Layers in contact with the coil, b) Entire tank

Figure 10 shows the temperature variables used in the coil model. As the coil is in contact with layers at different temperatures, it was vertically separated into four equal parts, each in contact with one layer. It was considered that the water leaves the coil at a temperature T_{cin}.

The model of the tank in POLYSUN considers losses to the atmosphere, therefore a new term regarding this effect was added to the Simulink model.

The final equations of the system based on [40] and [39] are summarized in Table 1, where $\dot{Q}coil = U_{coil}A_{coil}(T_j - T_{cini})$ is the heat transferred in the coil, $\dot{Q}loss = U_{loss}A_{loss}(T_j - T_a)$ the heat lost to the atmosphere, $\dot{Q}c1 = \frac{k_{j1}A_c}{\Delta x}(T_{j+1} - T_j)$ the heat exchanged by conduction with the lower layer, $\dot{Q}c2 = \frac{k_{j2}A_c}{\Delta x}(T_{j-1} - T_j)$ the heat exchanged by conduction with the upper layer.

The variables k_{j1} and k_{j2} are the thermal conductivity, which are given by the conductivity of the water times a tunable parameter and a difference of temperature when the tank is not stratified (model from [39] to correct the stratification), and equal to the conductivity of the water when the tank is stratified.

$$k_{j1} = \begin{cases} k_{j1}\Delta|T_{j+1} - T_j| & if\ T_j < T_{j+1} \\ k_{j1} & else \end{cases} \tag{4.6}$$

$$k_{j2} = \begin{cases} k_{j2}\Delta|T_{j-1} - T_j| & if\ T_{j-1} < T_j \\ k_{j2} & else \end{cases} \tag{4.7}$$

Table 1 - Equations for the temperature in each layer of the tank

Temperature in the layer	Equation
1	$$\rho c_p V_{tank} \frac{dT}{dt} = \rho c_p \dot{V}_t \left(T_{j+1} - T_j\right) - \dot{Q}loss + \dot{Q}c1 \quad (4.8)$$
2-4,9-11	$$\rho c_p V_{tank} \frac{dT}{dt} = \rho c_p \dot{V}_t \left(T_{j+1} - T_j\right) - \dot{Q}loss + \dot{Q}c1 + \dot{Q}c2 \quad (4.9)$$
5-8	$$\rho c_p V_{tank} \frac{dT}{dt} = \rho c_p \dot{V}_t \left(T_{j+1} - T_j\right) - \dot{Q}loss + \dot{Q}c1 + \dot{Q}c2 - \dot{Q}coil \quad (4.10)$$
12	$$\rho c_p V_{tank} \frac{dT}{dt} = \rho c_p \dot{V}_t \left(T_{in} - T_j\right) - \dot{Q}loss + \dot{Q}c2 \quad (4.11)$$

Equation 4.12 represents the temperature of the water returning to the solar collector, which is calculated as being in contact with the coil of the tank.

$$\rho c_p V_{coil} \frac{dT_{cin(i)}}{dt} = \rho c_p \dot{V}_c \left(T_{cin(i-1)} - T_{cin(i)}\right) + \dot{Q}coil \quad (4.12)$$

4.1.1.3 Validation procedure

The software used for the validation was POLYSUN, as it is one of the most used commercial software and has already been validated in the literature.

The validation was focused on two elements: the solar collector and the tank. The solar collector model used in POLYSUN was a flat plate collector, with a volume of 3L and an aperture area of $8m^2$. The tank model used had 500L, a coil heat exchanger, one entry, and one exit and included isolation.

A pump was integrated into the system to connect and control the flowrate between the solar collector and the tank. An on-off controller for the pump was implemented, with the pump switched on whenever the outflow temperature of the solar collector was higher than the temperature of the last layer in contact with the fluid in the coil.

The validation process requires the same conditions in both software tools (Simulink and POLYSUN). Therefore, the weather conditions and the characteristics of the simulated components had to be equal in the two simulations. The Simulink model needs the exterior temperature and the irradiance for the solar collector model. The weather files for the exterior temperature used were obtained from Meteonorm [41], as this is the data source used in POLYSUN. POLYSUN has procedures to calculate the irradiance onto the solar collector taking into account its tilt angle. This value of the irradiance already corrected for the specific tilt angle considered was used as input for the Simulink model, instead of the global irradiance from weather data (Meteonorm).

Regarding the demand profile, a typical hot water demand was selected from POLYSUN templates and considered in Simulink as well, as the solar collector together with the tank without backup are not able to exchange a large amount of energy, without lowering significantly the outflow temperature. The template demand profile was in the form of an hourly flowrate profile, while the return water had a fixed temperature value of 20ºC in both programs. The same heat demand was considered in both software. The heat delivered by the system through the hot water was calculated using Equation 4.13. When the outflow temperature of the tank (T_{tout}) is different between the two programs, the flowrate ($\dot{m}$) compensates the difference for them to have the same heat transfer (same demand).

$$\dot{Q} = \dot{m}c_p(T_{tout} - 20) \tag{4.13}$$

The model in POLYSUN and Simulink are represented respectively in Figure 11 and Figure 12.

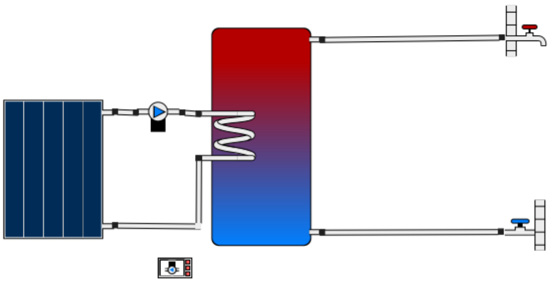

Figure 11 - Thermal system made in POLYSUN

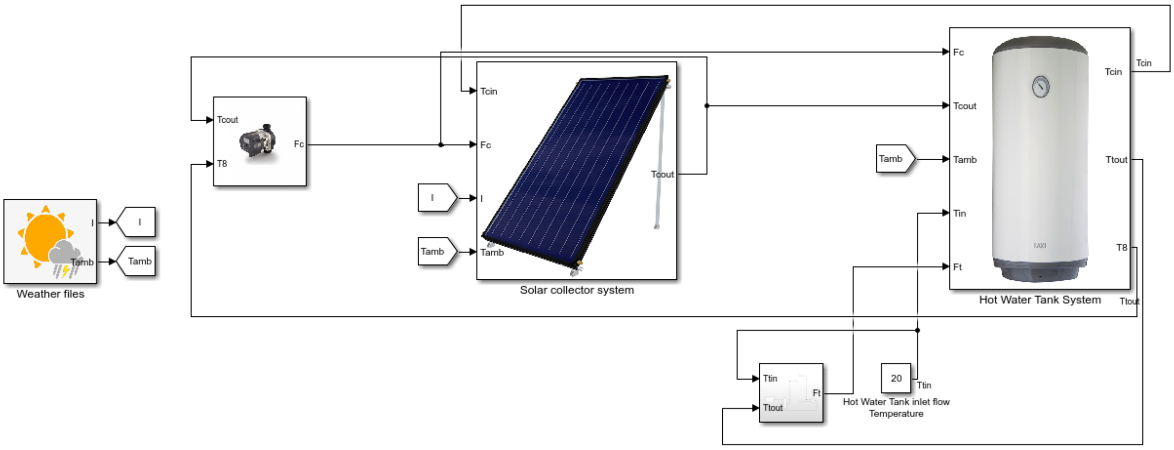

Figure 12 - Thermal system made in Simulink/Matlab for validation

4.1.2 Fan coil

A fan coil is used to exchange heat between the water system and the building. The air inside the building enters the fan coil, as well as the water from the tanks. Inside the fan coil, heat between the air and water is transferred and the air temperature increases/lowers allowing for the heating/cooling of the space with the outflow air of the fan coil.

4.1.2.1 Initial model

A fan coil model was previously performed by [38] following Equations 4.14 to 4.16.

$$\rho_a {c_p}_a V_a \frac{dT_{aout}}{dt} = \rho_a {c_p}_a \dot{V}_a (T_{ain} - T_{aout}) - U_{fc} A_{fc} (T_{aout} - T_{wout}) - \dot{Q}_{loss} \tag{4.14}$$

$$\rho_w {c_p}_w V_w \frac{dT_{wout}}{dt} = \rho_w {c_p}_w \dot{V}_w (T_{win} - T_{wout}) - U_{fc} A_{fc} (T_{wout} - T_{aout}) \tag{4.15}$$

$$\dot{Q}_{loss} = h A_o (T_{aout} - T_{building}) \tag{4.16}$$

4.1.2.2 New model

As will be shown in Chapter 5, by analyzing the equations and the results from POLYSUN, a better agreement with the results obtained with this software was achieved by considering some modifications. These included changes in the average temperature of the air to account for the losses to the outside of the fan coil and in the temperature used for the heat transferred between the air and the water. The log mean temperature was used to calculate this heat, considering the fan coil as a heat exchanger. The new model implemented for the fan coil is represented by the following equations:

$$\rho_a {c_p}_a V_a \frac{dT_{aout}}{dt} = \rho_a {c_p}_a \dot{V}_a (T_{ain} - T_{aout}) + UA\Delta T_{lm} - \dot{Q}_{loss} \tag{4.17}$$

$$\rho_w {c_p}_w V_w \frac{dT_{wout}}{dt} = \rho_w {c_p}_w \dot{V}_w (T_{win} - T_{wout}) - UA\Delta T_{lm} \tag{4.18}$$

$$\Delta T_{lm} = \frac{\Delta T_1 - \Delta T_2}{\ln(\Delta T_1 / \Delta T_2)} \tag{4.19}$$

$$\Delta T_1 = T_{hi} - T_{co} = T_{win} - T_{aout} \tag{4.20}$$

$$\Delta T_2 = T_{ho} - T_{ci} = T_{wout} - T_{ain} \tag{4.21}$$

$$\dot{Q}_{loss} = hA_o \left(\frac{T_{ain} + T_{aout}}{2} - T_{building}\right) \tag{4.22}$$

4.1.2.3 Validation procedure

POLYSUN was also used for the validation process of the fan coil. The system created using this software is displayed in Figure 13 and consisted of the previously validated system (solar collector and tank), the fan coil, and a building. The building was considered as a low energy building from POLYSUN and the control of the pump between the fan coil and the tank was performed to have a constant flowrate always circulating.

The fan coil model in POLYSUN has a nominal air flowrate of 42l/s and a nominal water flowrate of 73l/h, which values were also used for the flowrates in Simulink. As validation was only performed regarding the fan coil, the indoor temperature of the building from POLYSUN was used as an input to

Simulink for the air inlet temperature in the fan coil. The system implemented in Simulink is represented in Figure 14.

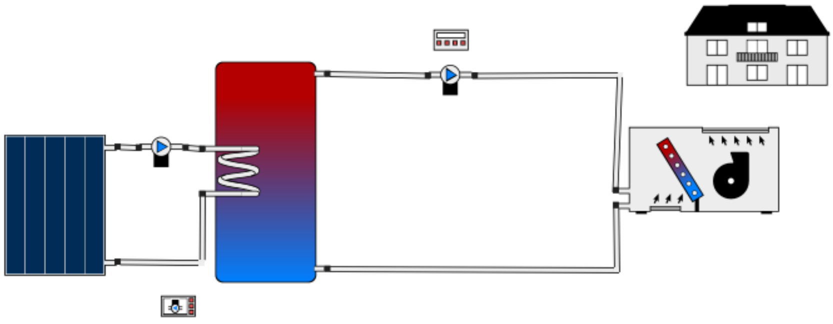

Figure 13 - Thermal system with a fan coil implemented in POLYSUN

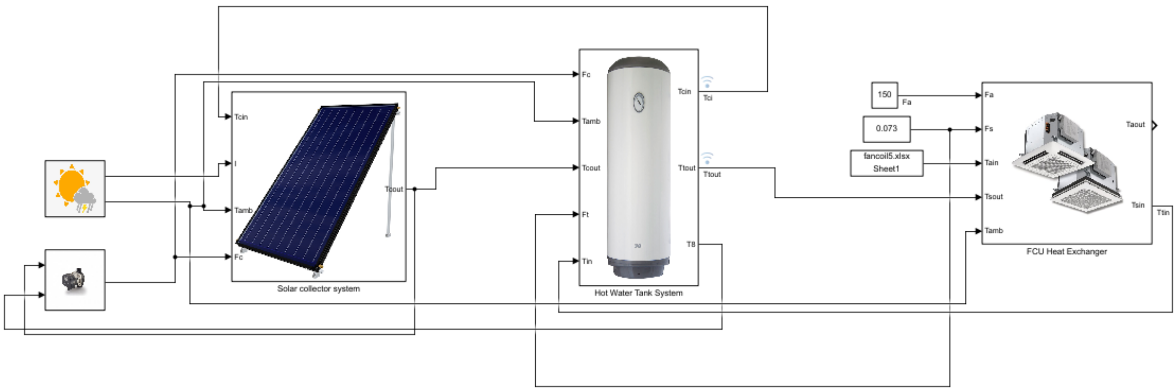

Figure 14 - Thermal system with a fan coil implemented in Simulink/Matlab

4.2 Heat Pump

Two options are available to model the heat pump: empirical and mathematical models. For the mathematical models, the equations representing the working principle of the heat pump are used, in contrast with the empirical model where the main parameters of the heat pump are modeled using measured values in specific conditions. An empirical model was considered in this thesis, as the mathematical model is too complex for the purpose of this study and required information not available. A datasheet was provided by the manufacture with the information necessary to the empirical model, such as the heat transferred (power of the heat pump) and the electrical power with different ambient temperatures (air inlet) and different outlet water temperatures.

The empirical model was done in Simulink and consisted of an interpolation process. The tables from the manufacture were uploaded to Matlab and for each state (water and air temperature), the heat and electrical power were interpolated.

The tables provided had values according to EN 14511 standard. These values were obtained using a fixed water temperature difference (between the inlet and outlet of the heat pump) of 5ºC. Consequently, the water flowrate circulating through the heat pump changes with the temperatures in the heat pump, and therefore it is also calculated in the model. The performance maps with the data from the manufacture are represented in Figure 15 and Figure 16, for heating and cooling respectively.

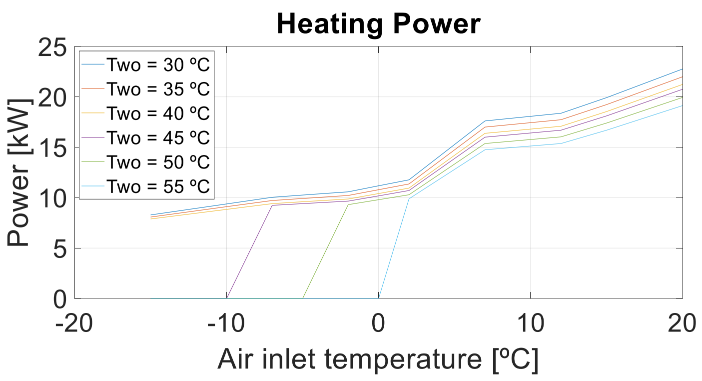

a)

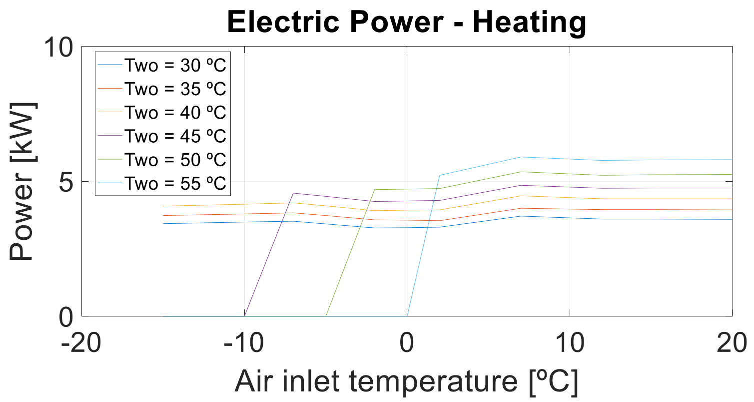

b)

Figure 15 – Heat Pump performance maps for heating with Two being the outflow temperature of the water, a) Heating Power, b) Electric Power

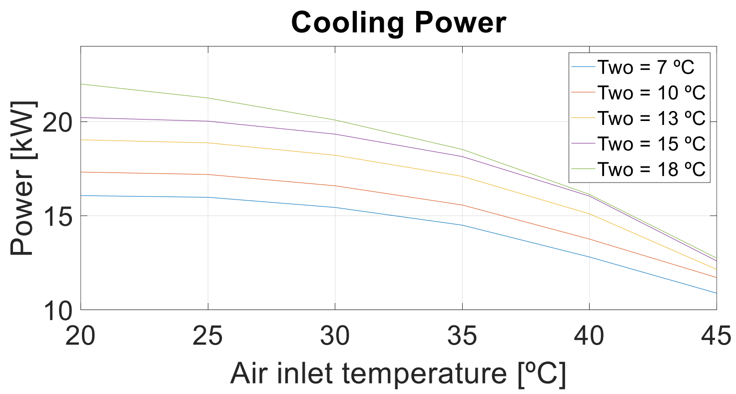

a)

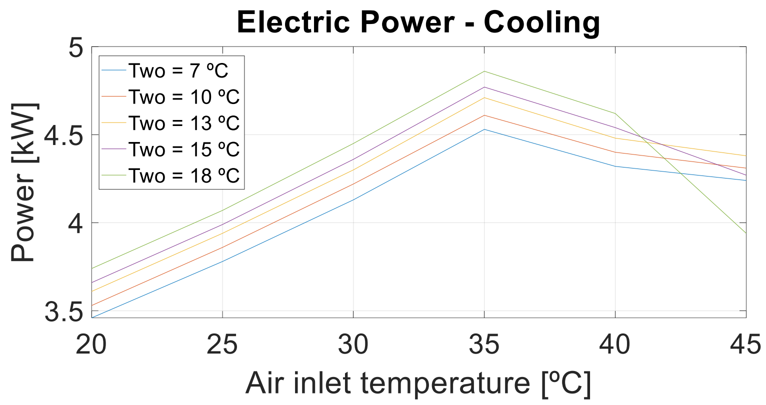

b)

Figure 16 - Heat Pump performance maps for cooling, a) Cooling Power, b) Electric Power

4.3 Global System

The global system simulated in this work is represented in Figure 17, including a solar collector, two tanks (hot water tank and storage tank), a heat pump and fan coils. The configuration in winter and summer are similar although they have some important differences. In winter, the solar collector is connected to the hot water tank by a solar system pump, while in summer the connection of the solar collector to the system is switched off. The water leaving the hot water tank can flow, in both seasons, directly to the storage tank, passing through the tank pump, or can flow through the heat pump where extra heat/cold is given. After that, the water leaves the storage tank to exchange heat with air from the rooms, through the five fan coils, returning then to the tank. The difference between seasons in this process is the position of extraction from the tanks. In winter, the water leaves the hot water tank from the top layer, as the interest of the system is to have high temperatures. The exit of the storage tank is, also, at the top and the return of the water for both tanks is at the bottom. In summer, as the goal is to have a low temperature in the tank, the exit of the tanks is at the bottom layer, and then the water returns and enters at the top. The temperatures used to control the pumps are also different in the two seasons.

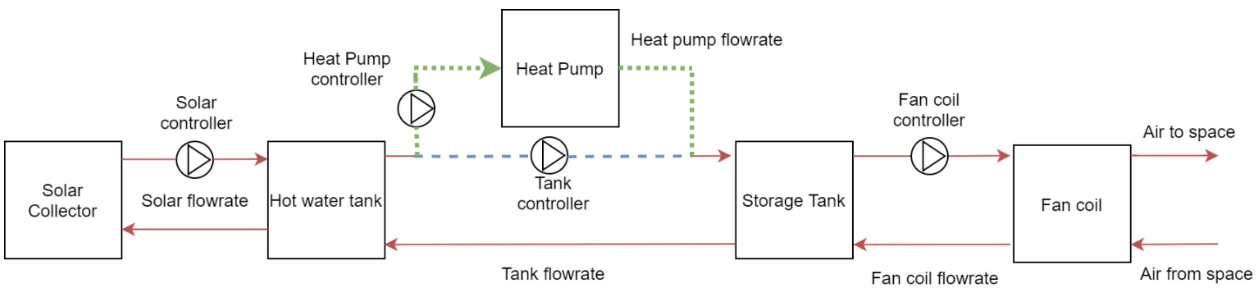

Figure 17 - Configuration of the global thermal system simulated

In order to model the global system, small changes had to be done to some of the previous individual models developed in the validation process. The characteristics of the models, both geometric and thermodynamic, were adapted to match the ones from the LNEG Pilot plant.

The solar collector used in the validation was similar to the one used in LNEG. The differences were only on the values of the size and efficiency, which are listed in Table 2.

Table 2 - Characteristics of the elements of the thermal system in LNEG – Solar collector

Solar collector	
$\boldsymbol{\eta_0}$	0,770
$\boldsymbol{U_{L1}}$	3,50 W/m^2K
$\boldsymbol{U_{L2}}$	0,0170 W/m^2K
$\boldsymbol{A}$	2,00 m^2
$\boldsymbol{V}$	0,00190 m^3

The hot water tank in the Pilot plant is slightly different from the one modeled due to the coil location. The coil in the tank used in LNEG is in contact with the layers in the middle and bottom of the tank, while the one simulated is vertically centered in the tank. The value of the U_{loss} was equal to the value used in the validation as the isolation materials are similar to the ones from the model used in POLYSUN. The properties of the hot water tank are presented in Table 3. The storage tank has the same configuration as the hot water tank, apart from the dimensions and characteristics of the coil (listed in Table 3). It was considered that both tanks were installed in a room with a fixed temperature of 20ºC.

Table 3 - Characteristics of the elements of the thermal system in LNEG - Tanks

	Hot water tank	**Storage tank**
$\boldsymbol{V}$	0,300 m^3	1,00 m^3
$\boldsymbol{V_{coil}}$	0,0101/8 m^3	0,0193/8 m^3
$\boldsymbol{U_{coil}}$	250 W/m^2K	250 W/m^2K
$\boldsymbol{A_{coil}}$	1,50/8 m^2	2,70/8 m^2
$\boldsymbol{U_{loss}}$	0,500 W/m^2K	0,250 W/m^2K
$\boldsymbol{H}$	1,50 m	2,00 m
$\boldsymbol{D}$	0,500 m	0,800 m

Three different sizes of the fan coil were modeled to satisfy the necessities of the three types of spaces. The decision of the flowrate and the size of the fan coils were made based on choosing a medium fan coil for Room 2. With these values for the fan coil in Room 2, an extrapolation was done, based on the respective dimensions of the spaces, to determine the characteristics of the other fan coils. For Room 1, $950\ m^3/h$ of air were considered, $250\ m^3/h$ for Room 2, and $125\ m^3/h$ for Rooms 3, 4, and 5.

4.3.1 Building

The model used in this thesis for the building was based on the model [38]. The model is described by the following equation:

$$\rho c_p V_i \frac{dT_i}{dt} = \rho c_p \dot{V}_{HVAC}\left(T_{aout(i)} - T_i\right) - U_{ext}A_{ext}(T_i - T_a) - \sum_{i=1}^{N_r} U_{int}A_{int}(T_i - T_k) + \rho c_p \dot{V}_{vent}(T_a - T_i) + \dot{q} \tag{4.23}$$

The equation represents the energy balance of the space. The accumulation of energy in the space depends on the heat transferred by the fan coil, the heat exchanged between the room and the exterior and between the room and the other rooms in contact with it, the ventilation of new air, and the heat generation inside the room.

The necessary flowrate of new air was considered to be $24\ m^3/h$ per person, as suggested in [42]. This air enters the room at ambient temperature to dilute the pollutants in the space under consideration.

4.4 Control

4.4.1 On-Off Control

The on-off control implemented consisted of the switch on-off of the eight pumps in the system. For the pumps of the system, the decision was made based on temperature difference, therefore the control is considered differential. As mentioned before, the value of the temperatures used for the control of the pumps differs in winter and summer.

Starting with the winter season, the criteria to control the pumps are listed in Table 4 and Table 5.

The solar system pump is controlled by the difference between the outflow water temperature of the solar collector and the temperature of the bottom layer of the tank. The values were chosen based on the information available in the literature. For the control of the tank pump, the difference between the temperature at the exit of the hot water tank and the bottom temperature of the storage tank was used. It was decided to use the same temperature difference considered in the solar system pump. For the heat pump, the difference between the reference temperature of the storage tank and its temperature was used as the control variable. The pump switched on when the temperature of the storage tank was 5ºC lower than the reference temperature, which was chosen as being equal to 50ºC. An additional condition was considered for the heat pump controller. The pump only switched on if the hot water tank had the capacity to heat the storage tank, which means that the sum of the hot water tank temperature with the increase of temperature in the heat pump had to be higher than the temperature in the storage tank.

To prevent frequent switching on and off of the pumps, a minimum operation time was set. This value was equal to 0.1hour (6minutes) for all the pumps in the system, except for the pumps of the fan coils, where the operation time was not limited.

Table 4 - Criteria to switch on-off the pumps of the system

	Solar system pump controller	**Tank pump controller**	**Heat pump controller**
On	$T_{cout} - T_{12} > 5℃$	$T_{tout} - T_{s12} > 5℃$	$T_{ref} - T_{sout} > 5℃$
Off	$T_{cout} - T_{12} < 1℃$	$T_{tout} - T_{s12} < 1℃$	$T_{ref} - T_{sout} < -1℃$

The controller of the heating/cooling of the building is based on the hour of the day. It was considered that it was occupied from 8 am to 7 pm, when the control follows the conditions listed in Table 5 . Between 6 am and 8 am the system heated the space before the occupants arrive. This heating is made in order to bring the temperature of the space closer to the comfort zone. From 7 pm to 6 am, the comfort in the space is not as important and the constraints can be relaxed.

Table 5 - Criteria to switch on-off the heating of the rooms

	8am – 7 pm	**6 am – 8 am**	**7pm – 6 am**
On	$T_{space} < 21℃$	$T_{space} < 18℃$	$T_{space} < 15℃$
Off	$T_{space} > 24℃$	$T_{space} > 22℃$	$T_{space} > 22℃$

Regarding the summer season, the solar system pump is always off and the tank and heat pump controllers have the same switching conditions as in the winter, only changing the signal of the left terms in Table 4 and the layer of the storage tank used for the tank pump controller. In the summer, the layer used is the last one in contact with the fluid in the coil (Layer 5). Note that Ttout refers in the summer to the temperature of the bottom layer, as this is the outflow temperature. The chosen reference temperature for the heat pump in the summer was 10ºC. A new condition was set in the summer in order to prevent too low temperatures in the hot water tank. The heat pump is always switched off when the tank reached 7ºC.

The conditions used for the controller of the building are represented in Table 6. From 7 pm to 6 am, the cooling of the space is switched off due to the low exterior temperatures at night which help to decrease the temperature of the space. For the period between 6 am and 8 am, similarly to the winter, the system is controlled to cool the space before the occupants arrive.

Table 6 - Criteria to switch on-off the cooling of the rooms

	8am – 7 pm	**6 am – 8 am**	**7pm – 6 am**
On	$T_{space} > 24℃$	$T_{space} > 26℃$	-
Off	$T_{space} < 21℃$	$T_{space} < 23℃$	-

4.4.2 Model Predictive Control

A new control strategy was implemented for the solar system pump, in this case, Model Predictive Control. This strategy allowed the decision on the value of the solar system flowrate ($\dot{V}_c$) (either zero or its maximum value), based on an optimization cost function and the output of a linear system. The procedure applied is represented in Figure 18.

The linear model is used to simulate the evolution of the system for two cases: solar system pump on or off. This is calculated for each time step with the correspondent irradiance, ambient temperature, and the previous variables from the system. The temperature, which in this case is the outflow temperature of the hot water tank, for both options (on and off of the pump) is the output of the linear system and the input of the optimization problem. Note that, for simplicity, the system selects the best option for the current time step, not using the prediction of disturbances, as typically done in MPC.

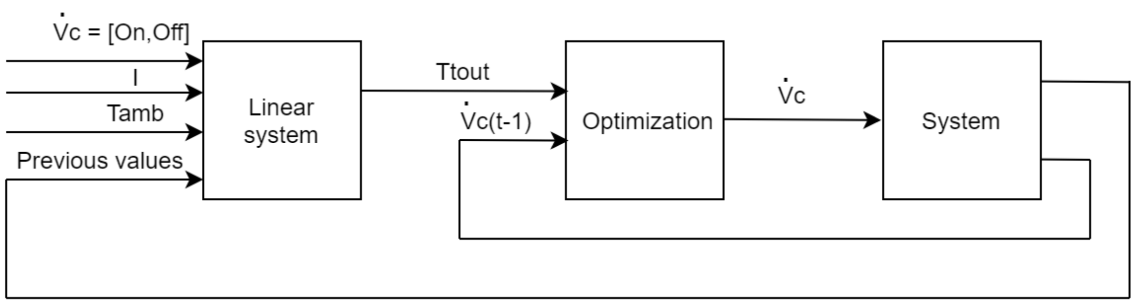

Figure 18 - Process used to apply MPC in the thermal system

For the application of MPC, both a linear model of the system and an optimization function were created.

As the system studied is nonlinear, a linearization procedure is needed to apply MPC. The toolboxes previously developed in MATLAB could not be used for this study, as they require either a linearization around a specific point (which is an incorrect approach as the system changes significantly with time) or a description of the system in equations (which was a very time consuming process).

For these reasons, the chosen method was to linearize the system through linear equations.

In order to obtain the linear system, a simpler model was created. The model consisted only of the solar collector and the hot water tank connected. These were the selected components, as they have a direct influence on the solar system flowrate. The influence of the other elements of the system was taken into account by the return temperature and flowrate to the hot water tank. This simplified model was run several times, with different input parameters, for a duration of 30 minutes each time. The input values were the solar system flowrate, irradiance, ambient temperature, previous temperature at the top layer of the tank, previous outflow temperature of the solar collector, previous flowrate between tanks, and previous inlet temperature in the tank. The values assumed for these variables are shown in Table 7.

Table 7 - Values used for the linearization of the system

	Values	Units
Solar system flowrate	[0,0.288]	m^3/h
Outflow temperature Solar collector	[10,30,50,70,90]	℃
Temperature of the tank	[10,30,50,70,90]	℃
Irradiance	[0,50,250,500,1000,1500]	W/m^2
Ambient temperature	[5,15,25]	℃
Flowrate between tanks	[0,2,3,4]	m^3/h
Water return temperature to the HW tank	[20,35,50]	℃

For each combination of the input values, the output of the system (T_{tout}) was saved. After having these values, a linear regression calculation function from Matlab was used. This function uses the values from the input parameters and relates them with the output variable, following Equation 4.24, with $t-1$ representing the previous value, $\dot{V}_t$ the flowrate between tanks and T_{tin} the return water temperature to the hot water tank.

$$T_{tout} = a_1 I + a_2 T_a + a_3 T_{tout(t-1)} + a_4 T_{tin(t-1)} + a_5 \dot{V}_{t(t-1)} + a_6 \qquad (4.24)$$

In order to obtain accurate results, the data was divided into specific conditions, due to the significant dynamics differences. The following conditions were used:

- T_{cout} is higher or lower than T_{tout} ($\Delta T > 0$ or $\Delta T < 0$) as it will influence the temperature of the tank increasing or decreasing with the flowrate;
- Irradiance is zero (night), or different from zero (day), which influences the temperature in the solar collector;
- Flowrate between the tanks and the solar system flowrate are zero or not, which has a significant influence on the tank temperature.

In total, the system was separated into 16 different options. These options were divided into 4 cases, listed in Table 8. Each case listed was then divided into four more cases, each one for a specific value of the two flowrates.

Table 8-Cases used for the linearization of the thermal system

Case	ΔT	I
1	< 0	$= 0$
2	> 0	$= 0$
3	> 0	$\neq 0$
4	< 0	$\neq 0$

After having the linear system, the optimization function was created.

The optimization problem consisted of a cost function that penalized the option that had a higher difference to the reference value and higher changes of flowrate with time (to prevent damage on the pump). The cost function used is represented in Equation 4.25, where w1 and w2 are the weights for the term of the temperature and variation of flowrate respectively, which were considered equal to 1 and 0.1. S1 and s2 are called size variables and are used to create dimensionless terms. The recommended values in the Matlab help page are the maximum amplitude of the signal. In this case, the temperatures varied between 40 and 70ºC in the tank, and the flowrate varied between 0 and 0.288. Therefore, $s1 = 70 - 40 = 30ºC$ and $s2 = 0.288$.

The reference temperature for the MPC controller considered was 85ºC, because it is a high temperature without reaching the 90ºC, maximum temperature allowed in the tank.

$$f(x) = \left(\frac{w_1}{s_1}(T - T_{refmpc})\right)^2 + \left(\frac{w_2}{s_2}\Delta\dot{V}\right)^2 , \Delta\dot{V} = \dot{V}_{c(t)} - \dot{V}_{c(t-1)} \qquad (4.25)$$

The global system implemented with MPC is represented in Figure 19.

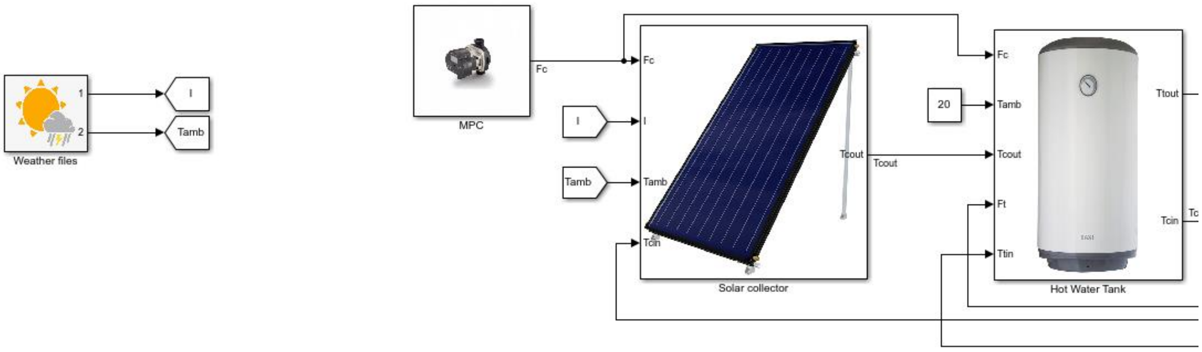

Weather files
I
Tamb
MPC
Fc
Solar collector
Tcin
Tcout
20
Ttout
Ft
Ttin
Hot Water Tank

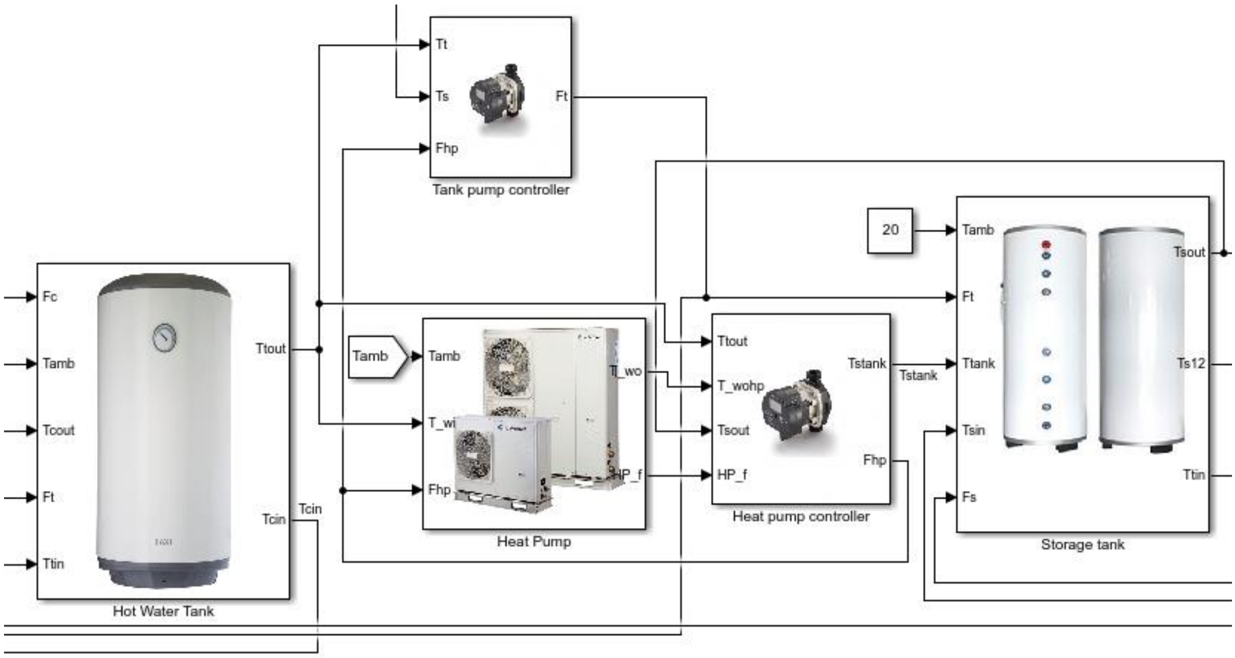

Tt
Ts
Fhp
Ft
Tank pump controller
Fc
Tamb
Tcout
Ft
Ttin
Ttout
Tcin
Hot Water Tank
T_wo
HP_f
Heat Pump
Ttout
T_wohp
Tsout
HP_f
Tstank
Fhp
Heat pump controller
20
Tank
Ttank
Tsin
Fs
Tsout
Ts12
Storage tank

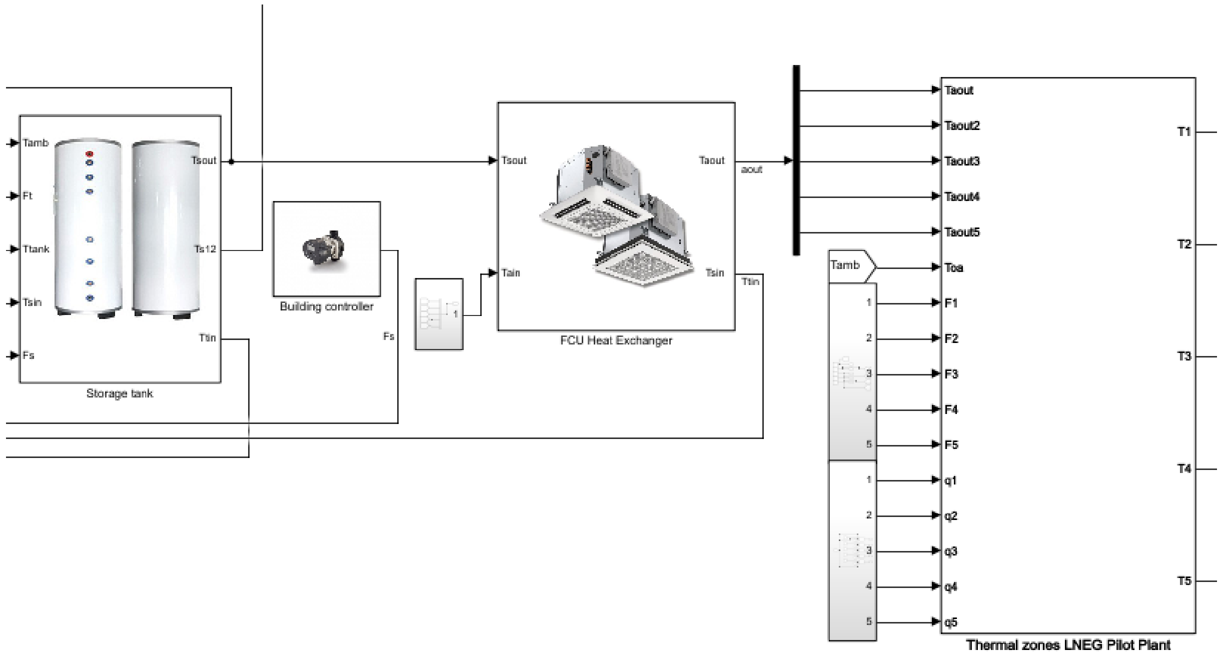

Figure 19 - System made in Simulink/Matlab

5 Results

In this chapter, the results of the validation process will be presented. Furthermore, the performance of the global system to heat/cool the spaces will be analyzed and parametric studies performed to investigate the impact of selected parameters on the system.

5.1 Validation

For a numerical comparison between POLYSUN and Simulink models, an error metric was applied. This metric was the root mean square error (RMSE) defined as:

$$RMSE = \sqrt{\frac{1}{n}\sum_{i=1}^{n}(\hat{y_i} - y_i)^2} \tag{5.1}$$

With y_i being the variable in Polysun and $\hat{y_i}$ in Simulink.

5.1.1 Solar collector and tank

Even after the modifications in the solar collector described in Chapter 4 (Equation 4.5), the validation of the initial model of the tank showed poor results. Significantly higher temperatures are obtained with the initial model in Simulink, that cannot be corrected by adding losses to the tank (not included in the initial model). This is illustrated in Figure 20, presenting the evolution of the tank temperature obtained with POLYSUN and Simulink, including losses in the tank.

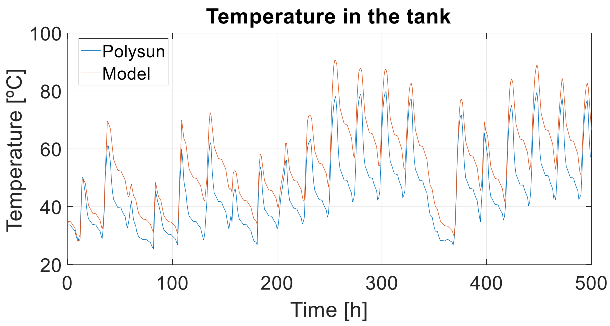

Figure 20 – Comparison between the initial model of the tank in POLYSUN and Simulink

The Simulink model developed by [38] for the tank simulated only the volume of the layers in contact with the coil heat exchanger, as a simplification of the model. This approach is not considered in POLYSUN, which models a stratified tank, and therefore, a new model of the tank was developed in Simulink. This model was done in an attempt to improve the performance of the initial model, considering the same stratification as in POLYSUN.

The comparison between the results of the two software tools with the stratified tank and the modifications in the solar collector is presented in Figures 21 to 23. It shows the evolution of three of the main variables in the summer and winter: the temperature of the top layer of the tank, the outflow temperature of the solar collector, and the useful heat in the solar collector. The periods selected for the graphs considered correspond to a part of January and July, which are representative of the winter and summer.

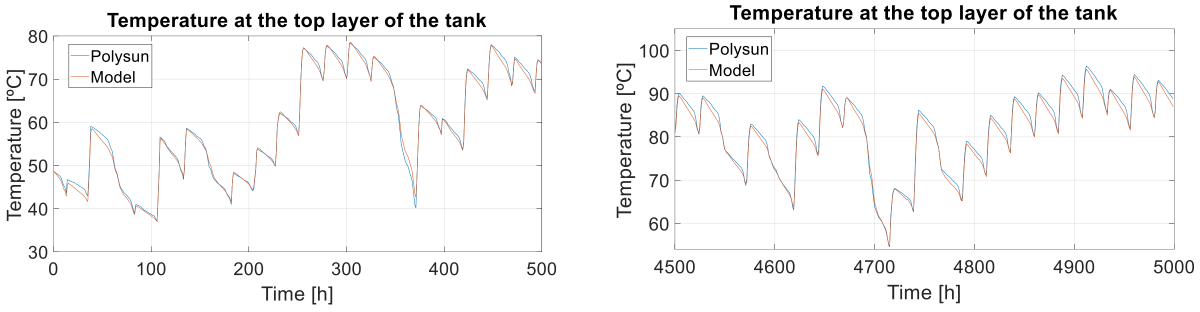

(a) (b)

Figure 21 – Comparison between the temperature in the tank of POLYSUN and Simulink, a) Winter, b) Summer

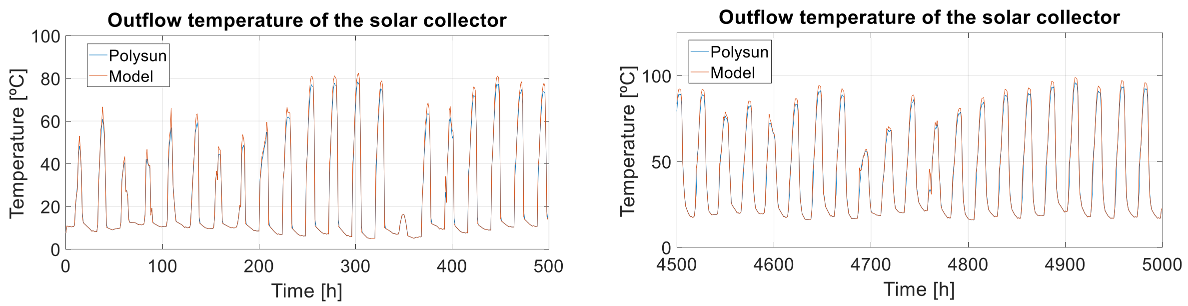

(a) (b)

Figure 22 - Comparison between the temperature of the solar collector of POLYSUN and Simulink, a) Winter, b) Summer

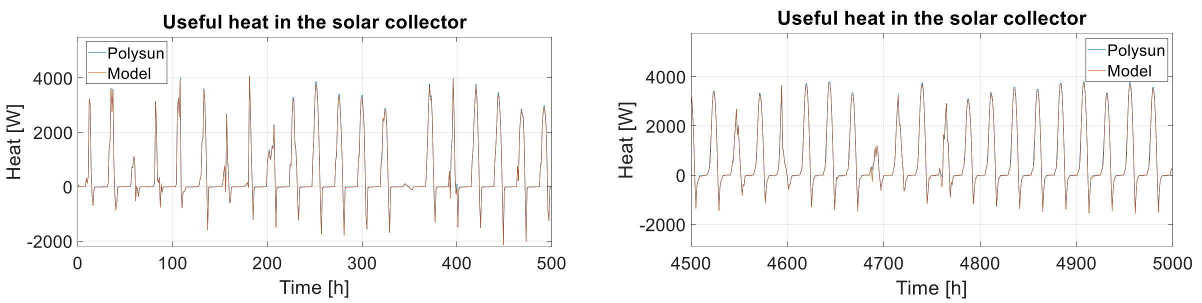

(a) (b)

Figure 23 - Comparison between the heat in the solar collector of POLYSUN and Simulink, a) Winter, b) Summer

As illustrated, the models implemented in Simulink reproduce the POLYSUN results with very good accuracy. The outflow temperature is sometimes overestimated, with a maximum deviation of 29% in the periods of highest irradiance. This effect could be related to differences in the equations used in POLYSUN (as they are not publically available, minor differences can exist in the equations and in the stratification method), to the calculation method for the coil used in POLYSUN, and to minor effects that were not modeled in Simulink, such as losses in connections, exits, and pump. In addition, the variable T_{cin} was compared with a variable in POLYSUN named "Temperature at the lower connection", but its exact measurement position in the tank is not known. Finally, the propagation of small errors may also contribute to the observed differences. Note that some errors arise in the comparison of the outflow temperature of the solar collector between the two software tools in the hours that the solar system flowrate switches on or off. This effect can be explained by small differences between T_{cout} and T_8 in both programs, which affect the time of switching the pump, then affecting the temperatures in this period. This error reaches a maximum deviation of 50% and disappears after the flowrate in both programs coincide, and the temperatures become significantly closer.

The error metric of the comparison between the results of the two software tools is presented in Table 9, following equations 5.1. As indicated, the errors are small, confirming the accuracy of the model implemented.

Table 9 – Error metric of the validation of the tank and solar collector

	RMSE
T_1 (°C) – Top Layer	1,05
T_5 (°C)	3,00
T_8 (°C)	2,08
T_9 (°C)	2,16
T_{cout} (°C)	2,38
T_{cin} (°C)	5,49
$\dot{Q}_c$ (W)	69,6

5.1.2 Fan coil

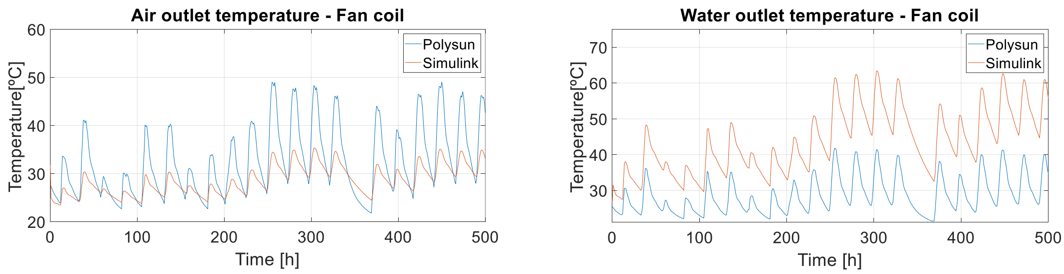

(a) (b)

Figure 24 – Initial comparison between the model of the fan coil in POLYSUN and Simulink, a) Air temperature, b) Water temperature

The validation of the initial model revealed significant differences with respect to the POLYSUN output as presented in Figure 24, showing the evolution of the air and water outlet temperature of the fan coil during a period in January.

The air and water outlet temperatures of the fan coil using the new improved model are displayed in Figure 25 to Figure 27, for a part of the months of January and November and in Table 10, are listed the errors metric for a comparison between POLYSUN and Simulink. The UA value was changed to better reproduce the results of POLYSUN.

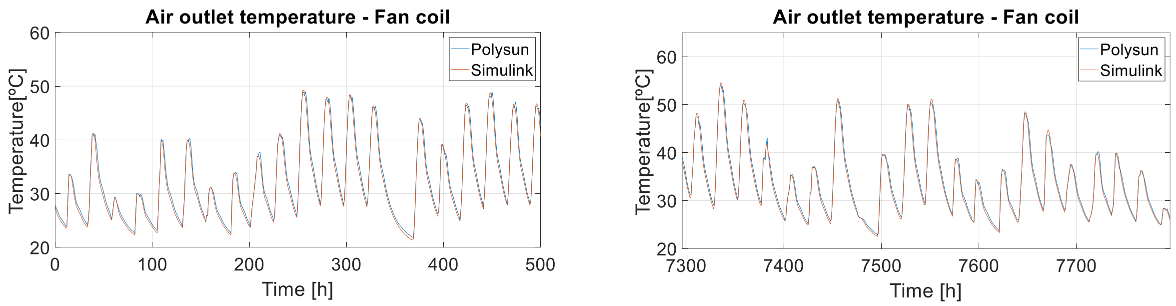

(a) (b)

Figure 25 - Comparison between the temperature of the air in the fan coil of POLYSUN and Simulink, a) January, b) November

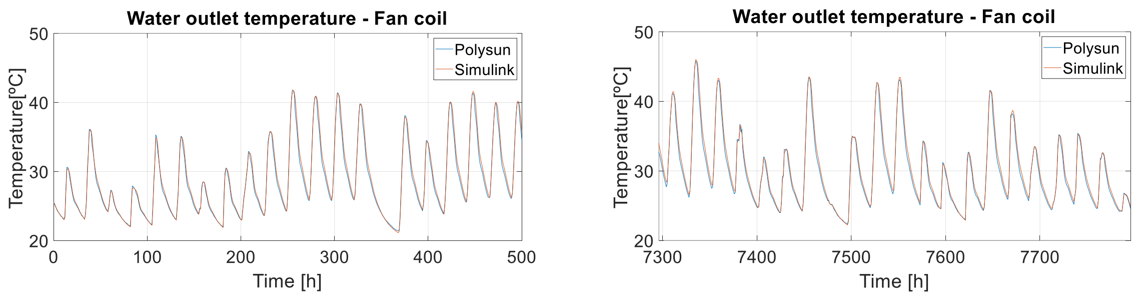

(a) (b)

Figure 26 - Comparison between the temperature of water in the fan coil of POLYSUN and Simulink, a) January, b) November

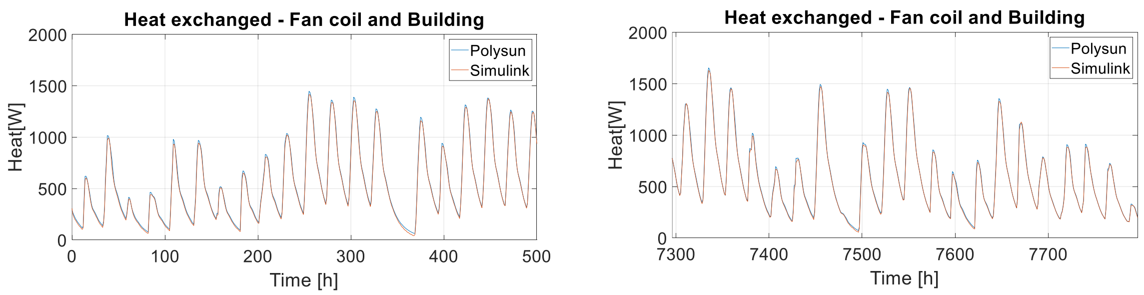

(a) (b)

Figure 27 - Comparison between the heat exchanged in the fan coil of POLYSUN and Simulink, a) January, b) November

Table 10 – Error metric of the validation of the fan coil

	RMSE
T_{aout} (℃)	0,996
T_{wout} (℃)	0,705
T_1 (℃)	0,475
$\dot{Q}_{fc}$ (W)	22,9
T_{cout} (℃)	1,79
$\dot{Q}_c$ (W)	46,2

Again, the new model implemented in Simulink reproduces with high accuracy the results provided by POLYSUN. In Table 10, are also compared the values for the previously validated components (solar collector and tank). The differences obtained could be associated with error propagation.

5.2 Comparison of On-Off Control and Model Predictive Control

As explained in Chapter 4, to apply MPC to the system, a linear model was developed.

The linearization of the system with the cases specified in Chapter 4 (Table 8) provided good results. Considering the difference between the value of T_{tout} obtained with the model and with the linearization, the highest error obtained was equal to 3.122% for case 3 with solar system flowrate and a flowrate between tanks. All the linear regressions had values of $R^2 > 0.9995$.

The results obtained with this more advanced control are now compared with those from the on-off control. Figure 28 presents the comparison of the evolution of the storage tank temperature, the hot water temperature, and the solar system flowrate obtained with the on-off and MPC controllers. The temperature obtained with on-off control is slightly higher than the one from MPC in the first days. After the first days, the temperature of the hot water tank differs in the two control methods due to differences in the solar system flowrate, influencing the temperature of the storage tank. Because of this difference, the heat pump switches on at different times in the two control methods, which, after some days, makes the comparison between the two systems not straight. Regarding the solar system flowrate, MPC has the advantage of not switching frequently the solar system pump at the beginning/end of the day, which could decrease the life of the pump.

The frequent switching of the pump is explained by the term $\rho c_p \dot{V}(T_{cin} - T_{cout})$ in Equation 4.1 starting to have values different from zero when the system begins to have solar system flowrate. The pump switches on when the temperature difference between the solar collector and the tank is larger than 5℃, and when there is no flowrate, T_{cin} is close to the temperature of the tank. In this situation, the term mentioned has a large negative value when the pump switches on and the outflow temperature of the solar collector decreases in a small amount of time. This process causes a frequent switching of the pump.

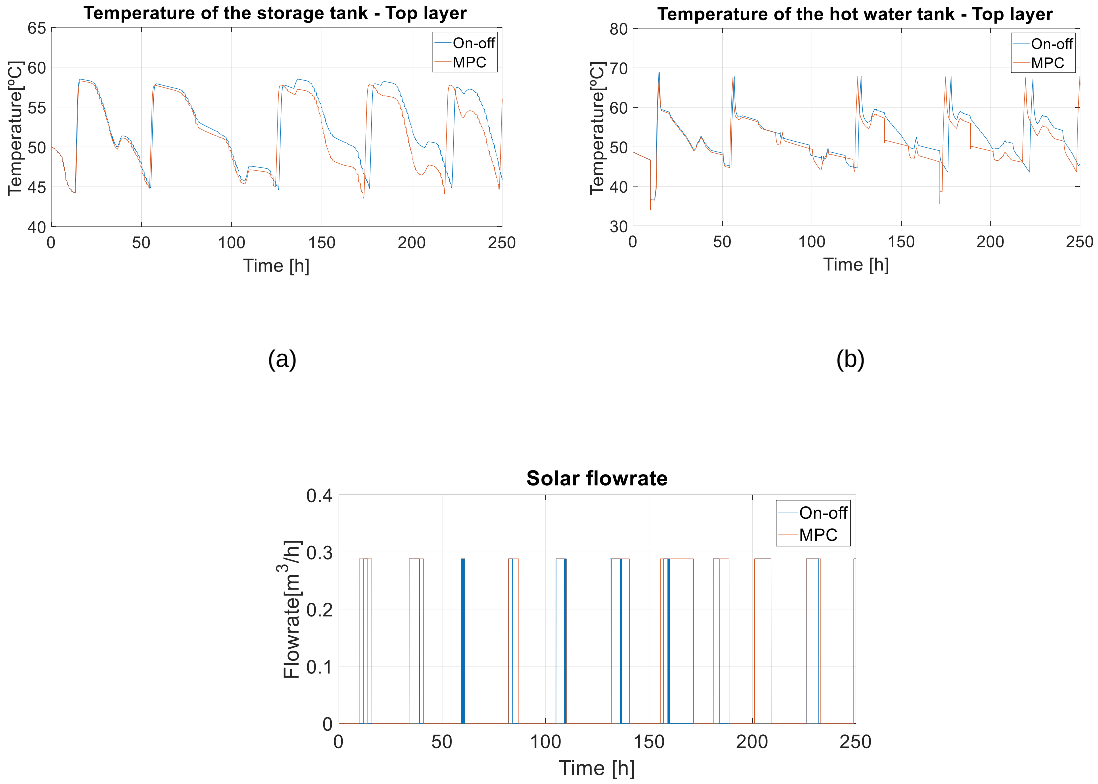

(a) (b)

(c)

Figure 28 – Comparison between On-off and MPC control for w2 = 0.1, a) Temperature of the storage tank, b) Temperature of the hot water tank, c) Solar system flowrate

In an attempt to improve the performance of the MPC controller, the weight of the variation of flowrate (w_2), which was previously set to 0.1, was decreased. When the first term of equation 4.25 is in the order of magnitude of the weight (w_2) squared, then the minimum of the optimization function can be affected and consequently influencing also the switching of the pump. Decreasing the weight decreases the importance given by the system to the variation of flowrate, and because of that, the solar system pump may switch off more frequently during operation.

As with $w_2 = 0.1$ the flowrate does not switch off during operation, this could indicate that excessive importance is given to the variation of the flowrate. The most favorable result was found with $w_2 = 0.01$ (see Figure 29). As illustrated, the temperature in the tank is practically equal to the one from on-off control. In Figure 30, a detail of the switching off during operation is presented. Although the MPC controller has instants when the pump switches off during operation (see Figure 30 b)), this effect happens only once a day (in opposite to the on-off control that, on the same day, switches on and off the pump several times).

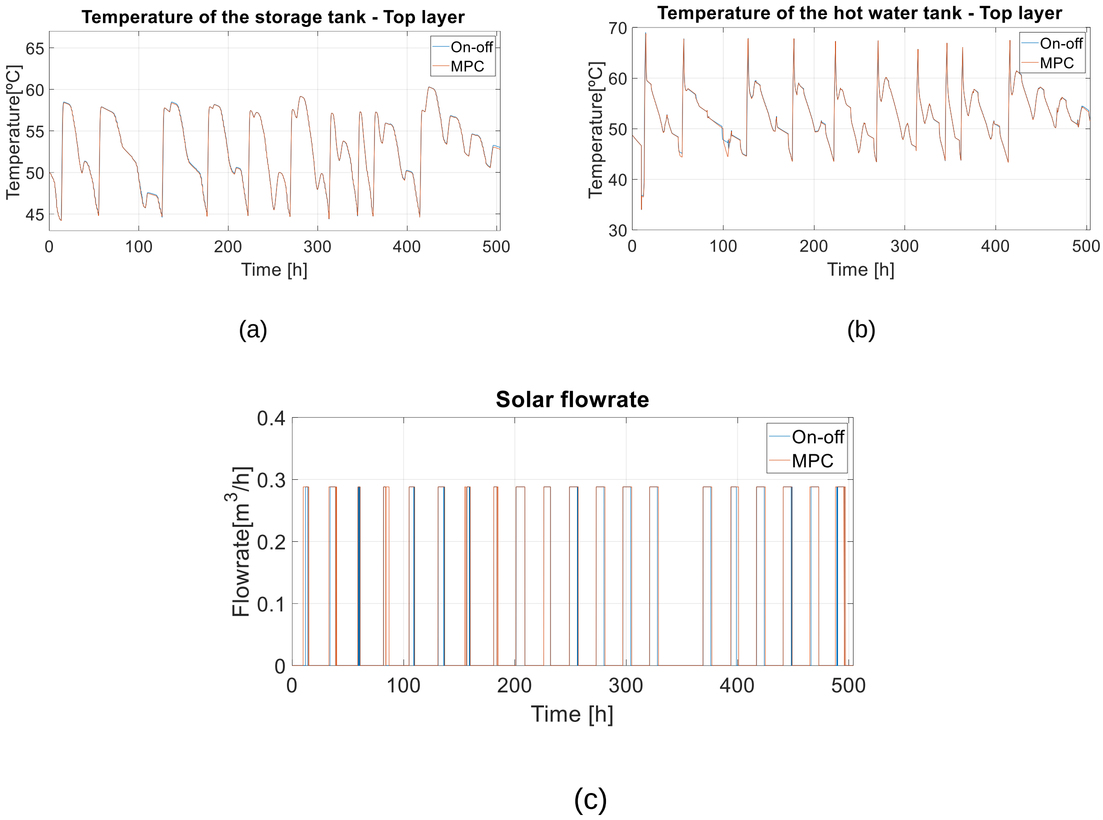

Figure 29 - Comparison between On-off and MPC control for w2 = 0.01, a) Temperature of the storage tank, b) Temperature of the hot water tank, c) Solar system flowrate

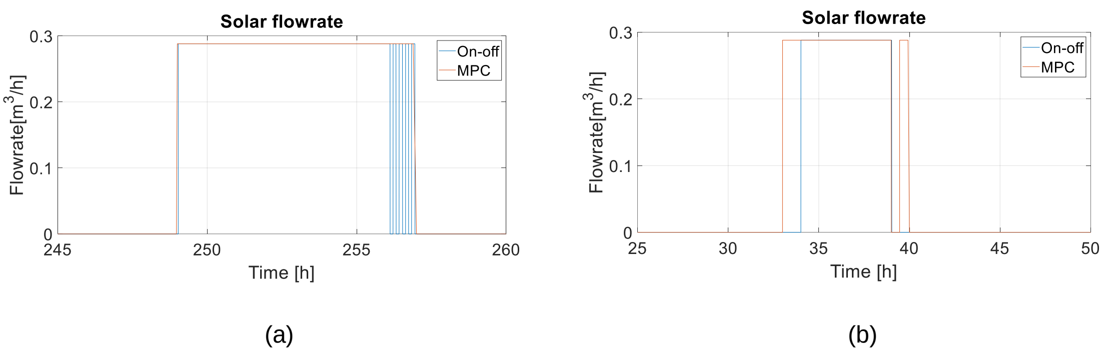

Figure 30 – Comparison between the solar system flowrate of On-off and MPC control, a) Switching off during operation of On-off, b) Switching off during operation of MPC

The impact of the control method on the temperature of the rooms is not significant. As it reaches a similar tank temperature to the one from on-off and switches less frequently the pump, the chosen control was MPC with a weight of 0.01.

5.3 System with Model Predictive Control – Winter

In this section, the evolution of the system with an MPC controller is further studied. Before analyzing the system, it is important to define the comfort zone considered. It was considered that the space is out of the comfort zone if $T_{space} > 25℃ \; or \; T_{space} < 20℃$, both in the winter and in the summer. The discomfort was only analyzed when the rooms were occupied. The evolution with MPC controller of the temperature in some of the rooms is represented in Figure 31, for the first three weeks of January, as well as for two days in this period.

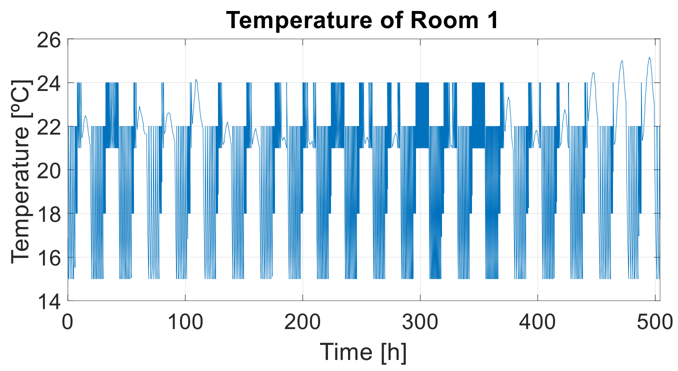

(a)

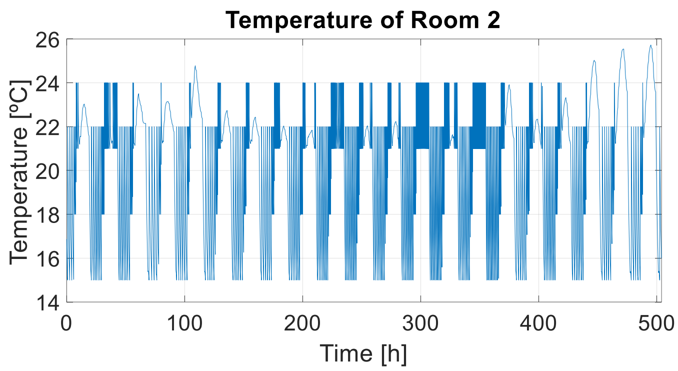

(b)

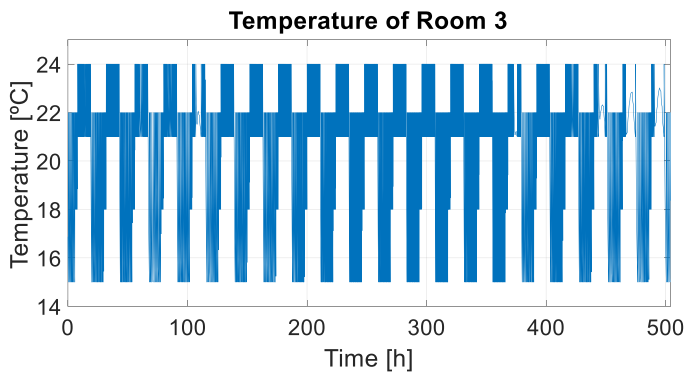

(c)

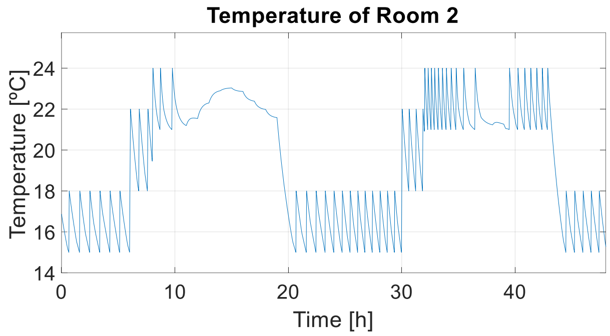

d)

Figure 31 – Performance of the system for heating in the Winter, a) Temperature of Room 1, b) Temperature of Room 2, c) Temperature of Room 3, d) Zoom of the temperature of Room 2

As illustrated, the system is able to provide heat for the space in all the rooms, keeping the temperatures in the comfort zone during the occupation period. Room 1, 2 and 5 reach high temperatures in the end of the three weeks, due to an excess of loads. Room 3 needs more heat than Room 4 and 5 because it has a larger area in contact with the exterior for the same occupation. The heat pump switches on only 11 times during the three weeks, consuming 122,9 KWh of electric energy.

5.4 System with On-Off Control – Summer

For the summer, the control strategy chosen was on-off, as the MPC was only applied to the solar system pump, which is switched off in the summer. The results of the system in the summer (three weeks in July and August) with on-off control are represented in Figure 32, showing the evolution of the temperature of Room 1 and 2 and the temperature of the bottom layer of the storage tank.

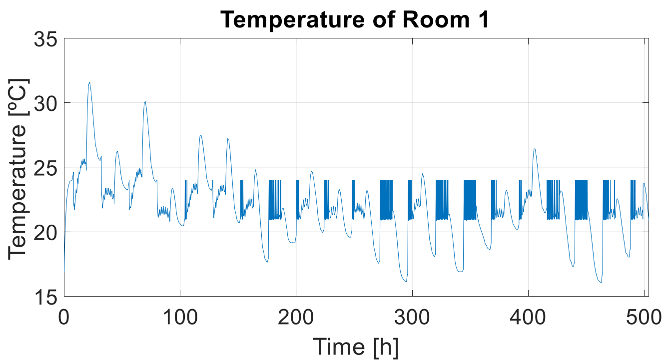

(a)

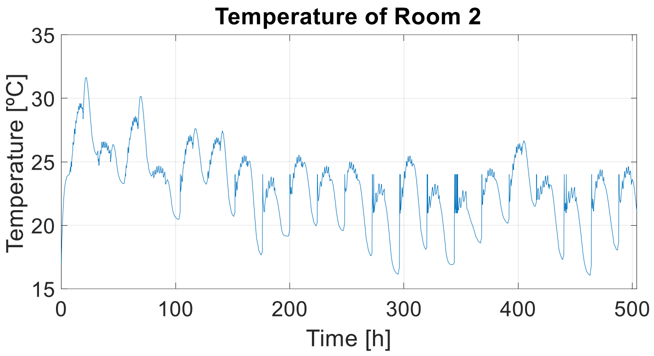

(b)

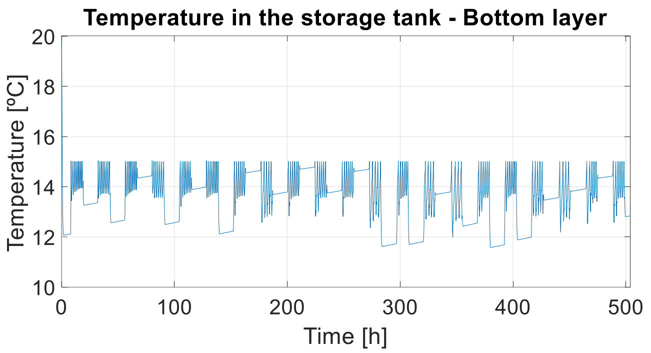

(c)

Figure 32 - Performance of the system for cooling in the Summer, a) Temperature of Room 1, b) Temperature of Room 2, c) Temperature in the storage tank

As illustrated, the system is able to keep the temperature of the rooms in the comfort zone for the majority of the time. Room 2 is the space with the worst cooling performance, having a significant amount of hours (13,15% of the occupation period) when the temperature is out of the comfort zone. This is due to an excess of thermal loads in the room, which will be varied in a parametric study. Room 3 is the second room with more discomfort, probably due to a higher area in contact with the exterior, than the other rooms of the same size. Room 1, 4, and 5 have approximately the same values of discomfort hours, which are not significant. It is important to note that the system does not have any cooling between 7 pm to 6 am, varying freely the temperature. During the night, the temperature of the space reaches values close to the exterior ambient temperature, as the only heat exchanged in the room during that period is the heat transfer through the exterior and interior walls. As in the summer, the ambient temperature at 7 pm can still have high values, there is an increase in temperature of the rooms after the cooling is switched off at those hours, reducing then during the night.

When the system is cooling the spaces, the temperature of the storage tank is most of the time equal to or lower than 15ºC, because the heat pump is controlled to switch on when the temperature of the tank is 5ºC higher than the reference (in this case 10ºC). As the only source of cooling is the heat pump, this device switches on and off every day and several times within the day, consuming 150,5 KWh of electric energy.

5.5 Parametric Studies

Having studied the behavior of the system in the winter and the summer for some specific conditions, parametric studies can now be performed to investigate the influence of relevant parameters of the system.

Three main variables were analyzed to compare the performance of the system in each study. Two variables related to the discomfort and the electric energy used in the heat pump were used. Regarding the measure of discomfort, the number of hours in discomfort during the occupation time (8 am-7 pm) and the product of the difference of the temperature of the space to the comfort zone and the time period out of the comfort zone (degree.hour of discomfort) were analyzed.

These were the chosen variables as the comfort of the space is the objective of the system and the electric energy used in the heat pump is the most significant external amount of energy necessary, except for the solar energy.

The studies were made for three weeks, both in the winter and summer, in order to have enough information without a large computational time.

Six studies were performed, three in the winter and three in the summer. The first study investigates the impact of heating the rooms at night. Having the heating system off during this period energy could be saved, but the consequence on the comfort and on the electric energy consumption of the heat pump at the beginning of the day require analysis. The location of the system was also changed from Lisbon to Madrid with the study performed both in the winter and the summer. Madrid has colder winters and hotter summers than Lisbon, and the impact of these weather conditions on the comfort was studied. Another study analyzed the increase in the solar collector area and its impact on the heat pump energy consumed in the winter. In the Summer, the reference temperature of the storage tank was varied to study the impact on the heat pump electric energy consumption, on the comfort, and on the temperature of the storage tank. Finally the occupation of Room 2 (always the room with more discomfort), was varied to study the impact on the discomfort.

5.5.1 Study 1: Heating during the night – Winter

This study analyses the influence of heating the rooms during the night. The initial condition consisted of heating the space when the temperature was below 15ºC and until it reached 22ºC. Changing these values will have an impact on the thermal system and on the temperature of the room. The three other options studied were: always switching off the heat during the night, heating between 15ºC and 18ºC, and between 18ºC and 22ºC. Figure 33 shows the discomfort hours and the degree.hour of discomfort of the rooms for the four options of heating considered and Table 11 summarizes the discomfort hours and the electric energy consumed by the heat pump.

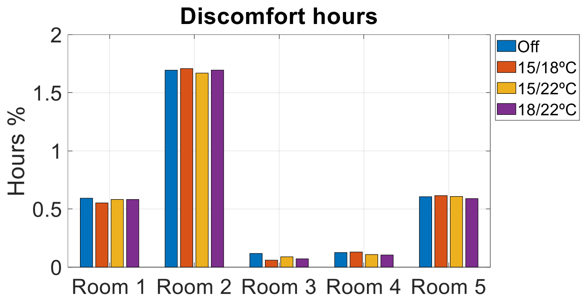

(a)

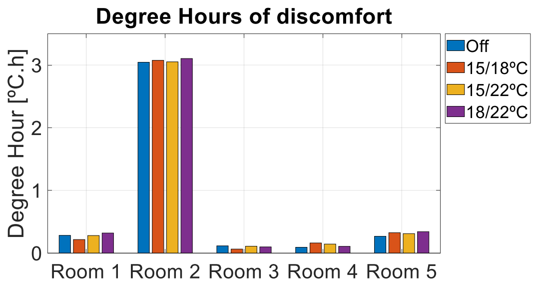

(b)

Figure 33 – Results of Study 1, a) Hours of discomfort, b) Degree.hour of discomfort

Table 11 - Results of Study 1 - Heating during night

	Discomfort hours %						**Electric Energy - Heat pump [KWh]**
	Room 1	**Room 2**	**Room 3**	**Room 4**	**Room 5**	**Average**	
Off	0,5931	1,6940	0,1176	0,1258	0,6061	0,6273	60,08
15/18℃	0,5527	1,7080	0,0603	0,1299	0,6153	0,6132	108,9
15/22℃	0,5824	1,6695	0,0890	0,1087	0,6080	0,6115	122,9
18/22℃	0,5820	1,6949	0,0719	0,1046	0,5898	0,6086	143,4

As the results show, the four options have a similar percentage of discomfort hours and degree.hour of discomfort during the night. The discomfort, in the majority of the time, happens when, at 8 am (beginning of the occupation time), the system was at a temperature below 20ºC, reaching rapidly the temperatures of comfort. The other type of discomfort is due to an excess of loads in the rooms, which brings the temperatures of the rooms to values above 25ºC. This effect causes the majority of the discomfort in Room 2, which is the room with more discomfort hours.

The electric energy consumption in the heat pump changes significantly between the cases considered, with the off option using less than half of the energy of the two last cases. This difference can be explained using Figure 34 that shows a zoom on the temperature of the top layer of the storage tank. The temperature of the storage tank decreases faster when the heating is on at night because it exchanges energy with the rooms, decreasing the temperature of the water that returns to the storage tank.

The Off option uses less electric energy from the fan coil pumps, as they are switched off during the night. As the Off option uses less electric energy and does not increase significantly the discomfort hours and the discomfort temperature, it was the chosen option.

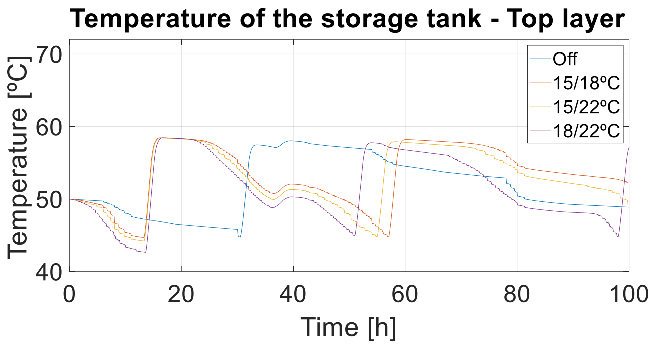

Figure 34 – Temperature of the storage tank for the cases in Study 1

5.5.2 Study 2: Location – Winter

To analyze the performance of the system with less favorable (in this case colder) weather conditions, a simulation was performed changing the building location to Madrid. The ambient temperature of Madrid and Lisbon is represented in Figure 35. As Madrid has a lower ambient temperature than Lisbon in the winter, it is expected that the system will need more electric energy from the heat pump to heat the spaces. The results of the study are presented in Figure 36 showing the discomfort variables and Table 12 summarizes the results of the discomfort hours and electric energy consumed by the heat pump.

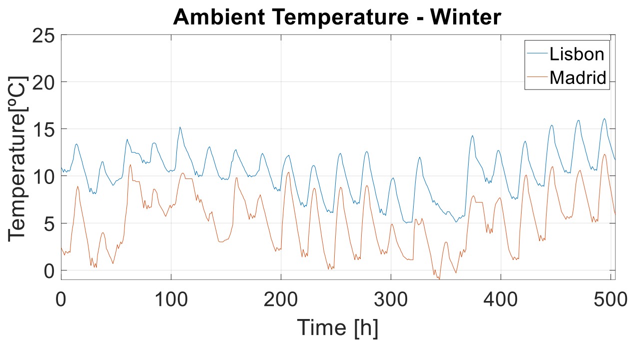

Figure 35 – Comparison between the weather conditions in Lisbon and Madrid

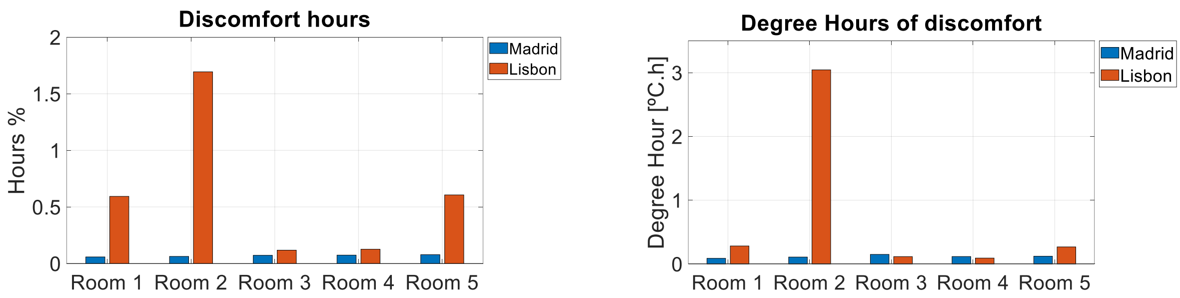

(a)

(b)

Figure 36 - Results of Study 2, a) Hours of discomfort, b) Degree.hour of discomfort

Table 12 - Results of Study 2 – Location, Winter

	Discomfort hours %						Electric Energy – Heat Pump [KWh]
	Room 1	**Room 2**	**Room 3**	**Room 4**	**Room 5**	**Average**	
Madrid	0,0580	0,0624	0,0721	0,0739	0,0779	0,0689	219,1
Lisbon	0,5931	1,6940	0,1176	0,1258	0,6061	0,6273	60,08

As predicted, the heat needed in Madrid is higher, leading to a faster decrease of the temperature in the storage tank, to a higher switching frequency of the heat pump, and to a higher electric heat pump energy consumption. The discomfort hours decreased, as some of these periods were related to an excess of internal loads in Lisbon. The degree.hour of discomfort in discomfort periods decreased or was at similar levels to Lisbon for all the rooms. The system in Madrid required a more frequent usage of the heating. As Madrid is colder in the Winter, the loads generated inside the building are compensated with higher losses to the outdoor and lower temperature of the inlet atmospheric air, which decreases the excess of loads, increasing the heat needed.

5.5.3 Study 3: Solar collector area - Winter

For this study, the on-off system was selected, as the linear system for the MPC was developed based on a specific value of solar collector area. Changing this parameter would require a new linear model of the plant, which would be traduced in a significant computational effort, not compensated by the small differences found between the on-off and MPC system.

The increase of the solar collector area would allow for a higher amount of energy transferred to the fluid and to a larger useful heat in the solar collector. With this, the temperature of the tank increases, requiring less energy from the heat pump. To analyze this effect, the area of the solar collector was increased by a factor of two, from 4 to $8m^2$. The temperature of the storage tank is shown in Figure 37.

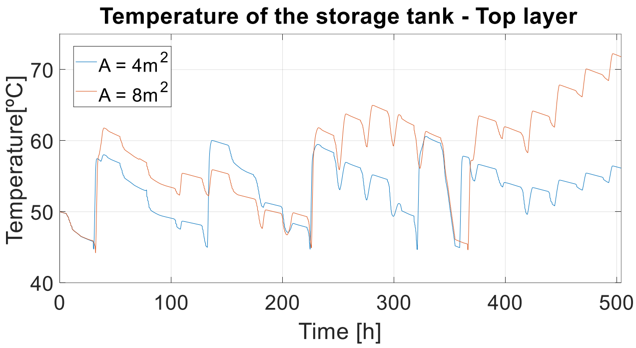

Figure 37 – Temperature of the storage tank in Study 3

The results are as expected, with the system absorbing more solar energy for the case with a larger collector area. The electric energy consumed by the heat pump is reduced from 61,39KWh to 36,88 KWh (60% less) as the collector area is increased by a factor of two. The comfort does not change significantly between the two cases, with a decrease in average for the case with a higher solar collector area.

5.5.4 Study 4: Reference temperature – Summer

The reference temperature is a parameter of the heat pump controller that is used to decide when to switch on or off the heat pump. This parameter has a direct influence on the temperature of the storage tank, which influences both the discomfort in the building and the electric power used in the heat pump. The reference temperature initially considered was 10ºC and in this study, 8ºC and 15ºC will also be analyzed. Lower reference temperatures were not studied due to the fast reach of significantly low temperatures at the outlet of the heat pump. The results regarding the discomfort are represented in Figure 38 and Table 13 summarizes the values of discomfort hours and energy consumption of the heat pump obtained in this study.

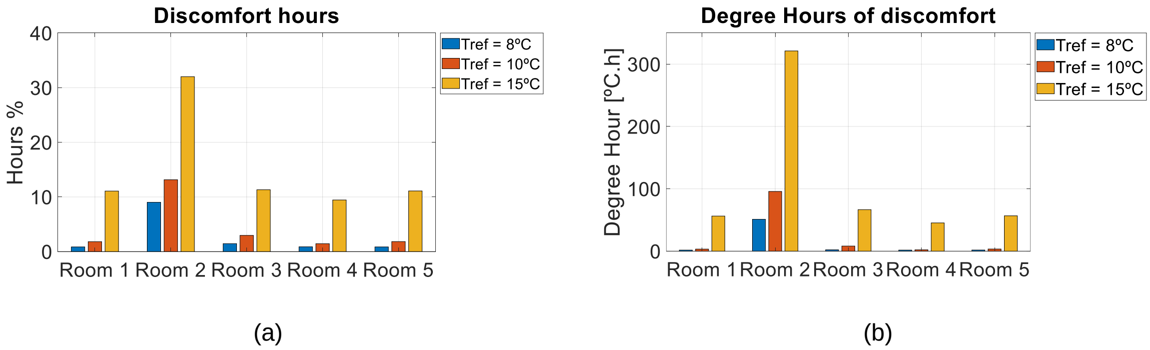

Figure 38 - Results of Study 4, a) Hours of discomfort, b) Degree.hour of discomfort

Table 13 - Results of Study 4 - Reference temperature, Summer

	Discomfort hours %						**Electric Energy – Heat Pump [KWh]**
	Room 1	**Room 2**	**Room 3**	**Room 4**	**Room 5**	**Average**	
8℃	0,8545	9,016	1,454	0,8754	0,8545	2,611	157,5
10℃	1,818	13,15	2,961	1,448	1,834	4,242	150,5
15℃	11,08	32,01	11,32	9,443	11,09	14,99	121,4

The system with a reference temperature of 8ºC has lower discomfort hours and lower degree.hour of discomfort. This happens because the temperature in the storage tank increases as the reference temperature increases (see in Figure 39).

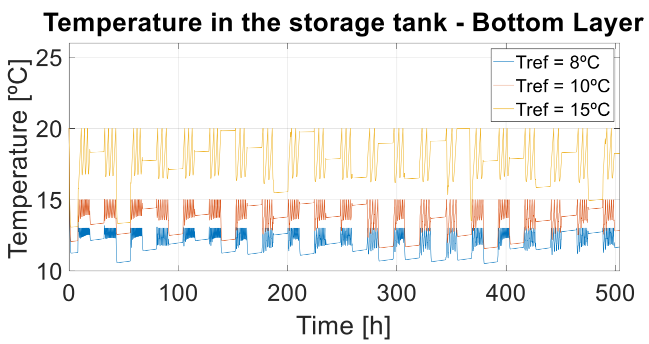

Figure 39 – Evolution of the temperature in the storage tank for the three cases in Study 4

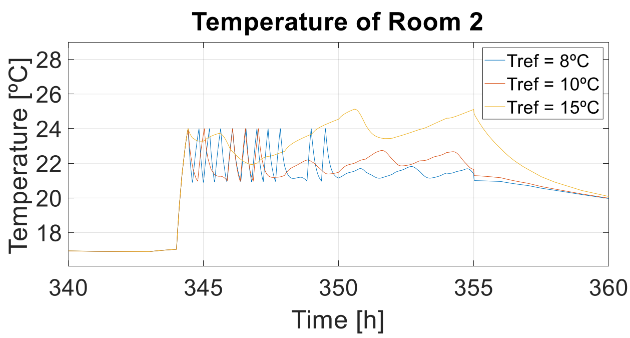

Figure 40 - Evolution of the temperature of room 2 for the three cases in Study 4

An interesting observation regarding the performance of the system is that, in some instants, the systems are not able to decrease the temperature of the rooms to 21ºC and the cooling continues for several hours on. The system with a reference temperature of 8ºC is able to bring the temperature of the rooms to 21ºC more often, (see Figure 40), as the temperature at the storage tank is lower.

The electric energy used by the heat pump for the system with a reference temperature of 8ºC is only 5% higher than the one with 10ºC as reference temperature while reducing the discomfort in all the rooms by 62% on average. Therefore, a reference temperature of 8ºC was considered the best scenario.

5.5.5 Study 5: Location – Summer

In this parametric study, the system location was changed to Madrid, that according to the data from POLYSUN, has a higher ambient temperature than Lisbon in the summer (see Figure 41). As a result, the cooling performance of the system is expected to be worse in Madrid, with more discomfort hours and higher temperatures in the rooms. Figure 42 and Table 14 show the discomfort parameters of this study and the electric energy consumption of the heat pump.

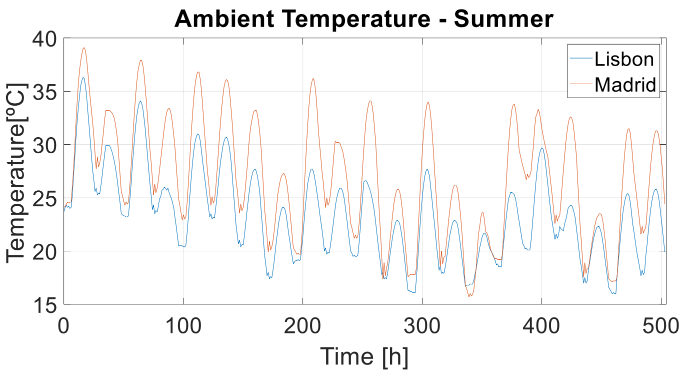

Figure 41 – Comparison between the ambient temperature in Lisbon and Madrid during Summer

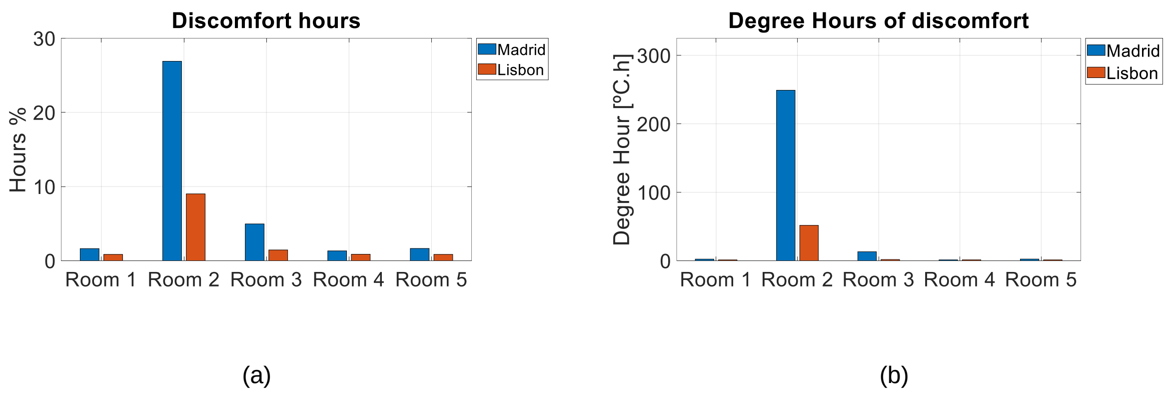

Figure 42 - Results of Study 5, a) Hours of discomfort, b) Degree.hour of discomfort

Table 14 - Results of Study 5 – Location, Summer

	Discomfort hours %						Electric Energy - Heat Pump [KWh]
	Room 1	**Room 2**	**Room 3**	**Room 4**	**Room 5**	**Average**	
Madrid	1,639	26,89	4,963	1,329	1,654	7,295	225,8
Lisbon	0,8545	9,016	1,454	0,8754	0,8545	2,611	157,5

As expected, Madrid has more discomfort hours in all the rooms, and an increase in the degree.hour of discomfort. This is related to the ambient temperature, which affects several parameters. The heat transferred through the walls and the temperature of the air entering the system to guarantee the ventilation needed, are the main parameters influenced by the ambient temperature. Regarding the electric energy needed by the heat pump, Madrid consumes more 43% than Lisbon, due to a higher frequency of switching on the heat pump and due to a higher instant power, as illustrated in Figure 43. This is related to the fact that, in the summer, the heat pump used in LNEG, has an increase of the electric power needed for increasing ambient temperatures, for the majority of the temperatures involved in the simulation.

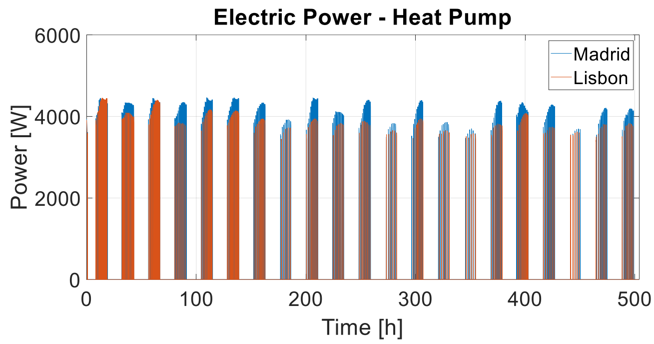

Figure 43 – Electric power consumed by the heat pump in Lisbon and Madrid

5.5.6 Study 6: Occupation of Room 2 - Summer

As Room 2 is the room with more discomfort in the summer, a parametric study was done where the occupancy of the room was changed, keeping the occupancy of the other rooms fixed. As it is a meeting room, it was considered that two, three, four, or five people could be in this space, being five the value previously used. The number of people was considered fixed for the period of study. The results are presented in Figure 44 and Table 15.

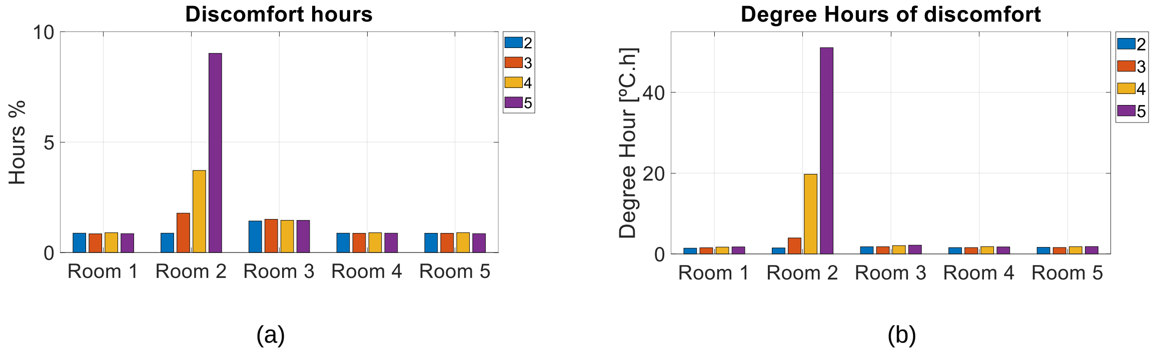

Figure 44 – Results of Study 6, a) Hours of discomfort, b) Degree.hour of discomfort

We observed that with a lower number of occupants in Room 2, the system is able to bring all the spaces to the comfort zone almost all the time studied. This is due to fewer loads in the room, which decreases the amount of cooling needed in the space. This change in the occupation of Room 2 does not have a significant impact on the temperature of the other rooms. The electric energy used by the heat pump reduces as the number of people reduces, as the loads inside the room decrease, decreasing the temperature of the air and decreasing the heat exchanged in the fan coil.

Table 15 – Results of Study 6 – Occupation of Room 2, Summer

	Discomfort hours %						**Electric Energy – Heat Pump [KWh]**
People	**Room 1**	**Room 2**	**Room 3**	**Room 4**	**Room 5**	**Average**	
2	0,8757	0,8757	1,426	0,8757	0,8726	0,9851	143,3
3	0,8463	1,782	1,502	0,8691	0,8691	1,174	148,4
4	0,8963	3,715	1,457	0,8963	0,8998	1,573	153,3
5	0,8545	9,016	1,454	0,8754	0,8545	2,611	157,5

6 Conclusions and Future work

This thesis consisted of the modeling of the thermal system located on LNEG Pilot Plant. The first objective was the validation of models of the solar collector, hot water tank and fan coil, which, after some modifications, was accomplished.

A complete integrated model constituted by a solar collector, two tanks, a heat pump, and fan coils, and with the objective of heating/cooling a building was implemented successfully, filling the gap in the literature of models in Simulink coupling solar thermal and air-water heat pumps for space heating. The system was able to keep the building in the comfort zone for the majority of the time. Two control strategies were studied, with MPC showing more stable results than the on-off control. The performance of the system was analyzed for different conditions with parametric studies implemented both in winter and summer.

This work showed that Simulink is a suitable software to model thermal systems and their control, due to its flexibility and its adaptability.

This thesis was only focused on the thermal system. An important upgrade would be to consider the integration with the electrical system, having decision making based on both systems. The heat pump is the main component affected by the proposed integration of the two systems, being necessary to develop a new control approach.

Some components of the Pilot Plant in LNEG are still being installed, therefore an experimental study and comparison with the simulated system were not possible. In the future, it would be interesting to compare the simulation results obtained with the experimental data.

A simplified MPC was implemented in this work. To have better results and a better control strategy, an increase of the complexity of MPC would be required, applying models of prediction of the disturbances (for example weather forecast).

REFERENCES

[1] “Edifícios.” https://www.dgeg.gov.pt/pt/areas-setoriais/energia/eficiencia-energetica/edificios/ (accessed Feb. 15, 2021).

[2] APA, “Plano Nacional Energia E,” *Plano Nac. Energ. E Clima 2021-2030 (Pnec 2030)*, pp. 1–200, 2019.

[3] “IMPROVEMENT » LNEG.” https://www.lneg.pt/en/project/improvement-2/ (accessed Feb. 15, 2021).

[4] “Heat – Renewables 2019 – Analysis - IEA.” https://www.iea.org/reports/renewables-2019/heat#abstract (accessed Mar. 09, 2021).

[5] W. Weiss and M. Spörk-Dür, “Solar Heat Worldwide 2020 - Global market development and trends in 2019,” *Sci. Technol. Built Environ.*, vol. 24, no. 8, pp. 819–819, 2019.

[6] Solar Heat Europe, “Solar Heat Markets in Europe,” no. November 2019, 2019.

[7] I. Sarbu and C. Sebarchievici, “A comprehensive review of thermal energy storage,” *Sustain.*, vol. 10, no. 1, 2018, doi: 10.3390/su10010191.

[8] R. Melicio and C. M. P. Cabrita, “Solar Thermal System — Practical Case Study,” no. November, 2011.

[9] “Heat Pumps: the New High-Tech Energy Source – LG HVAC STORY.” https://www.lghvacstory.com/heat-pumps-the-new-high-tech-energy-source/ (accessed Oct. 22, 2021).

[10] “EHPA Stats.” http://stats.ehpa.org/hp_sales/story_sales/ (accessed Mar. 02, 2021).

[11] “Key Facts on Heat Pumps - EHPA.” https://www.ehpa.org/technology/key-facts-on-heat-pumps/ (accessed Mar. 02, 2021).

[12] DGEG, “Balanço Energético,” 2019.

[13] G. H. Shi, L. Aye, D. Li, and X. J. Du, “Recent advances in direct expansion solar assisted heat pump systems: A review,” *Renew. Sustain. Energy Rev.*, vol. 109, no. January 2018, pp. 349–366, 2019, doi: 10.1016/j.rser.2019.04.044.

[14] A. Badiei *et al.*, “A chronological review of advances in solar assisted heat pump technology in 21st century,” *Renew. Sustain. Energy Rev.*, vol. 132, no. July, 2020, doi: 10.1016/j.rser.2020.110132.

[15] J. Cai, F. Zhang, and J. Ji, “Comparative analysis of solar-air dual source heat pump system with different heat source configurations,” *Renew. Energy*, vol. 150, pp. 191–203, 2020, doi:

10.1016/j.renene.2019.12.128.

[16] Z. Wang, P. Guo, H. Zhang, W. Yang, and S. Mei, "Comprehensive review on the development of SAHP for domestic hot water," *Renew. Sustain. Energy Rev.*, vol. 72, no. January, pp. 871–881, 2017, doi: 10.1016/j.rser.2017.01.127.

[17] D. Carbonell, M. Y. Haller, D. Philippen, and E. Frank, "Simulations of combined solar thermal and heat pump systems for domestic hot water and space heating," *Energy Procedia*, vol. 48, no. September, pp. 524–534, 2014, doi: 10.1016/j.egypro.2014.02.062.

[18] R. S. Kamel, A. S. Fung, and P. R. H. Dash, "Solar systems and their integration with heat pumps: A review," *Energy Build.*, vol. 87, pp. 395–412, 2015, doi: 10.1016/j.enbuild.2014.11.030.

[19] T. Sun *et al.*, "A novel solar-assisted ground-source heat pump (SAGSHP) with seasonal heat-storage and heat cascade utilization: Field test and performance analysis," *Sol. Energy*, vol. 201, no. March, pp. 362–372, 2020, doi: 10.1016/j.solener.2020.03.030.

[20] C. J. Banister and M. R. Collins, "Development and performance of a dual tank solar-assisted heat pump system," *Appl. Energy*, vol. 149, pp. 125–132, 2015, doi: 10.1016/j.apenergy.2015.03.130.

[21] S. R. Asaee, V. I. Ugursal, and I. Beausoleil-Morrison, "Techno-economic assessment of solar assisted heat pump system retrofit in the Canadian housing stock," *Appl. Energy*, vol. 190, pp. 439–452, 2017, doi: 10.1016/j.apenergy.2016.12.053.

[22] M. Pinamonti, I. Beausoleil-Morrison, A. Prada, and P. Baggio, "Water-to-water heat pump integration in a solar seasonal storage system for space heating and domestic hot water production of a single-family house in a cold climate," *Sol. Energy*, vol. 213, no. October 2020, pp. 300–311, 2021, doi: 10.1016/j.solener.2020.11.052.

[23] T. Long *et al.*, "Performance analysis and optimization of a solar-air source heat pump heating system in Tibet, China," *Energy Build.*, vol. 220, p. 110084, 2020, doi: 10.1016/j.enbuild.2020.110084.

[24] S. Poppi, C. Bales, M. Y. Haller, and A. Heinz, "Influence of boundary conditions and component size on electricity demand in solar thermal and heat pump combisystems," *Appl. Energy*, vol. 162, pp. 1062–1073, 2016, doi: 10.1016/j.apenergy.2015.10.190.

[25] J. Vega and C. Cuevas, "Parallel vs series configurations in combined solar and heat pump systems: A control system analysis," *Appl. Therm. Eng.*, vol. 166, no. May 2019, p. 114650, 2020, doi: 10.1016/j.applthermaleng.2019.114650.

[26] P. Jelínek, J. Sedlák, and B. Lišková, "Comparison of polysun simulation with direct measurements of solar thermal system in rapotice," in *Advanced Materials Research*, 2014, vol. 1041, pp. 158–161, doi: 10.4028/www.scientific.net/AMR.1041.158.

[27] "Welcome | TRNSYS : Transient System Simulation Tool." http://www.trnsys.com/#1 (accessed Jun. 14, 2021).

[28] C. Tzivanidis, E. Bellos, G. Mitsopoulos, K. A. Antonopoulos, and A. Delis, "Energetic and financial evaluation of a solar assisted heat pump heating system with other usual heating systems in Athens," *Appl. Therm. Eng.*, vol. 106, pp. 87–97, 2016, doi: 10.1016/j.applthermaleng.2016.06.004.

[29] E. Atam, "Current software barriers to advanced model-based control design for energy-efficient buildings," *Renew. Sustain. Energy Rev.*, vol. 73, no. August 2016, pp. 1031–1040, 2017, doi: 10.1016/j.rser.2017.02.015.

[30] S. Lim, S. Park, H. Chung, M. Kim, Y. J. Baik, and S. Shin, "Dynamic modeling of building heat network system using Simulink," *Appl. Therm. Eng.*, vol. 84, pp. 375–389, 2015, doi: 10.1016/j.applthermaleng.2015.03.068.

[31] F. Mosallat, T. Elmekkawy, D. L. Friesen, T. Molinski, S. Loney, and E. L. Bibeau, "Modeling, simulation and control of flat panel solar collectors with thermal storage for heating and cooling applications," *Procedia Comput. Sci.*, vol. 19, no. Seit, pp. 686–693, 2013, doi: 10.1016/j.procs.2013.06.091.

[32] M. Kiyan, E. Bingöl, M. Melikoğlu, and A. Albostan, "Modelling and simulation of a hybrid solar heating system for greenhouse applications using Matlab/Simulink," *Energy Convers. Manag.*, vol. 72, pp. 147–155, 2013, doi: 10.1016/j.enconman.2012.09.036.

[33] G. Aboina, M. A. Tankari, A. M. Tahir, and G. Lefebvre, "Analysis of the influences of internal heat loads on a solar heating system equipped with a heat pump," *Int. J. Renew. Energy Res.*, vol. 10, no. 3, pp. 1327–1333, 2020.

[34] A. Vallati, P. Ocłoń, C. Colucci, L. Mauri, R. de Lieto Vollaro, and J. Taler, "Energy analysis of a thermal system composed by a heat pump coupled with a PVT solar collector," *Energy*, vol. 174, pp. 91–96, 2019, doi: 10.1016/j.energy.2019.02.152.

[35] J. Deng, Z. Tian, J. Fan, M. Yang, S. Furbo, and Z. Wang, "Simulation and optimization study on a solar space heating system combined with a low temperature ASHP for single family rural residential houses in Beijing," *Energy Build.*, vol. 126, pp. 2–13, 2016, doi: 10.1016/j.enbuild.2016.05.019.

[36] F. Behrooz, N. Mariun, M. H. Marhaban, M. A. M. Radzi, and A. R. Ramli, "Review of control techniques for HVAC systems-nonlinearity approaches based on fuzzy cognitive maps," *Energies*, vol. 11, no. 3, 2018, doi: 10.3390/en11030495.

[37] T. Ferhatbegovic, P. Palensky, G. Fontanella, and D. Basciotti, "Modelling and design of a linear predictive controller for a solar powered HVAC system," *IEEE Int. Symp. Ind. Electron.*, pp. 869–874, 2012, doi: 10.1109/ISIE.2012.6237203.

[38] I. S. Técnico, “IMPROVEMENT SUDOE INTERREG EU Project -DELIVERABLE D3.2.1. Report on Technical Specification of the IMPROVEMENT heating and cooling system.” .

[39] A. L. Nash, A. Badithela, and N. Jain, “Dynamic modeling of a sensible thermal energy storage tank with an immersed coil heat exchanger under three operation modes,” *Appl. Energy*, vol. 195, pp. 877–889, 2017, doi: 10.1016/j.apenergy.2017.03.092.

[40] A. Rahman, N. Fumo, and A. D. Smith, “Simplified modeling of thermal storage tank for distributed energy heat recovery applications,” *ASME 2015 9th Int. Conf. Energy Sustain. ES 2015, collocated with ASME 2015 Power Conf. ASME 2015 13th Int. Conf. Fuel Cell Sci. Eng. Technol. ASME 2015 Nucl. Forum*, vol. 2, no. June, 2015, doi: 10.1115/ES2015-49170.

[41] “intro - Meteonorm (en).” https://meteonorm.com/en/ (accessed Sep. 15, 2021).

[42] E. e S. S. Ministérios do Ambiente, Ordenamento do Território e Energia e da Solidariedade, “Portaria n.º 349-D/2013 de 2 de dezembro dos Ministérios do Ambiente, Ordenamento do Território e Energia e da Solidariedade, Emprego e Segurança Social,” *Diário da República*, no. 40, p. 34, 2013.